Open access • Journal Article • DOI:10.1038/NG.3921

Heterogeneity of neuroblastoma cell identity defined by transcriptional circuitries

— Source link

Valentina Boeva, Valentina Boeva, Caroline Louis-Brennetot, Agathe Peltier ...+32 more authors

Institutions: PSL Research University, Centre national de la recherche scientifique, Curie Institute, Aix-Marseille University ...+7 more institutions

Published on: 24 Jul 2017 - Nature Genetics (Nature Research)

Topics: Neuroblastoma

Related papers:

- Neuroblastoma is composed of two super-enhancer-associated differentiation states
- The genetic landscape of high-risk neuroblastoma
- Multipotent peripheral glial cells generate neuroendocrine cells of the adrenal medulla
- Super-Enhancers in the Control of Cell Identity and Disease
- Selective gene dependencies in MYCN-amplified neuroblastoma include the core transcriptional regulatory circuitry.

Share this paper:

View more about this paper here: https://typeset.io/papers/heterogeneity-of-neuroblastoma-cell-identity-defined-by-oszwhplohz

Heterogeneity of neuroblastoma cell identity defined by transcriptional circuitries

Valentina Boeva, Caroline Louis-Brennetot, Agathe Peltier, Simon Durand, Cecile Pierre-Eugene, Virginie Raynal, Heather Etchevers, Sophie Thomas, Alban Lermine, Estelle Daudigeos-Dubus, et al.

▶ **To cite this version:**

Valentina Boeva, Caroline Louis-Brennetot, Agathe Peltier, Simon Durand, Cecile Pierre-Eugene, et al.. Heterogeneity of neuroblastoma cell identity defined by transcriptional circuitries. Nature Genetics, Nature Publishing Group, 2017, 49 (9), pp.1408-1413. 10.1038/ng.3921 . hal-01741718

HAL Id: hal-01741718
https://hal.archives-ouvertes.fr/hal-01741718

Submitted on 26 Mar 2018

HAL is a multi-disciplinary open access archive for the deposit and dissemination of scientific research documents, whether they are published or not. The documents may come from teaching and research institutions in France or abroad, or from public or private research centers.

L'archive ouverte pluridisciplinaire **HAL**, est destinée au dépôt et à la diffusion de documents scientifiques de niveau recherche, publiés ou non, émanant des établissements d'enseignement et de recherche français ou étrangers, des laboratoires publics ou privés.

Heterogeneity of neuroblastoma cell identity revealed by transcriptional circuitries

Authors: Valentina Boeva[1,2,*], Caroline Louis-Brennetot[3], Agathe Peltier[3], Simon Durand[3], Cécile Pierre-Eugène[3], Virginie Raynal[3,4], Heather Etchevers[5], Sophie Thomas[6], Alban Lermine[1], Estelle Daudigeos-Dubus[7], Birgit Geoerger[7], Martin F. Orth[8], Thomas G. P. Grünewald[8], Elise Diaz[9,10], Bertrand Ducos[9,10,11], Didier Surdez[3], Angel M. Carcaboso[12], Irina Medvedeva[2], Thomas Deller[13], Valérie Combaret[14], Eve Lapouble[15], Gaelle Pierron[15], Sandrine Grossetête-Lalami[3], Sylvain Baulande[4], Gudrun Schleiermacher[3,16,17], Emmanuel Barillot[1], Hermann Rohrer[13], Olivier Delattre[3], and Isabelle Janoueix-Lerosey[3,*]

* Corresponding authors

Affiliations

[1]Institut Curie, PSL Research University, Inserm U900, Mines-ParisTech, F-75005, Paris, France.

[2]Institut Cochin, Inserm U1016, CNRS UMR 8104, University Paris Descartes UMR-S1016, F-75014, Paris, France.

[3]Institut Curie, PSL Research University, Inserm U830, F-75005, Paris, France.

[4]Institut Curie Genomics of Excellence (ICGex) Platform, Institut Curie Research Center, F-75005, Paris, France.

[5]Aix Marseille Univ, Inserm, GMGF, UMR S910, F-13005, Marseille, France.

[6]Inserm U1163, Laboratory of Embryology and Genetics of Congenital Malformations, Paris Descartes - Sorbonne Paris Cité University, Imagine Institute, F-75015 Paris, France.

[7]Vectorology and Anticancer Therapies, UMR 8203, CNRS, Univ. Paris-Sud, Gustave Roussy, Université Paris-Saclay, F-94805, Villejuif, France.

[8]Max-Eder Research Group for Pediatric Sarcoma Biology, Institute of Pathology, LMU Munich, Thalkirchner Str. 36, 80337 Munich, Germany.

[9]High Throughput qPCR facility, IBENS, PSL Research University, 46 rue d'Ulm, F-75005,

30 Paris, France.
31 [10]LPS-ENS, UPMC, Université Denis Diderot, CNRS UMR 8550, PSL 24 rue Lhomond, F-
32 75005, Paris, France.
33 [11]Laser Microdissection Facility, CIRB Collège de France, Place Marcellin Berthellot, F-75005,
34 Paris, France.
35 [12]Institut de Recerca Sant Joan de Deu, 08950 Barcelona, Spain.
36 [13]Institute for Clinical Neuroanatomy, Goethe University, D-60590, Frankfurt/M, Germany.
37 [14]Centre Léon Bérard, Laboratoire de Recherche Translationnelle, Lyon, France.
38 [15]Institut Curie, Unité de Génétique Somatique, F-75005, Paris, France.
39 [16]Laboratory RTOP (Recherche Translationnelle en Oncologie Pédiatrique), laboratoire
40 "Gilles Thomas", Institut Curie, F-75005, Paris, France.
41 [17]Department of translational research, Institut Curie, F-75005, Paris, France.
42
43

44 Neuroblastoma is a tumor of the peripheral sympathetic nervous system[1], derived from
45 multipotent neural crest cells (NCCs). To define Core Regulatory Circuitries (CRCs) controlling
46 the gene expression program of neuroblastoma, we established and analyzed the neuroblastoma
47 super-enhancer landscape. We discovered three types of identity in neuroblastoma cell lines: a
48 sympathetic noradrenergic identity defined by a CRC module including the PHOX2B, HAND2
49 and GATA3 transcription factors (TFs); an NCC-like identity, driven by a CRC module
50 containing AP-1 family TFs; a mixed type further deconvoluted at the single cell level.
51 Treatment of the mixed type with chemotherapeutic agents resulted in enrichment of NCC-like
52 cells. The noradrenergic module was validated by ChIP-seq. Functional studies demonstrated
53 dependency of neuroblastoma with noradrenergic identity on PHOX2B, evocative of lineage
54 addiction. Most neuroblastoma primary tumors express TFs from the noradrenergic and NCC-
55 like modules. Our data demonstrate a novel aspect of tumor heterogeneity relevant for
56 neuroblastoma treatment strategies.
57

58 **Keywords**: neuroblastoma, neural crest cells, ChIP-seq, super-enhancers, core regulatory
59 circuitries, transcription factors, cell proliferation
60

61 Nearly one in six patients who die of a childhood cancer had a neuroblastoma, a tumor of
62 the peripheral sympathetic nervous system[1]. Several genes including *MYCN*[2], *ALK*[3–6] and
63 *TERT*[7,8] have been shown to act as major drivers of neuroblastoma oncogenesis. In this work, we
64 have determined the core transcriptional regulatory circuitries (CRCs)[9] that govern the gene
65 expression program of neuroblastoma. CRCs, which can be defined by super-enhancer (SE)
66 mapping of H3K27 acetylation mark (H3K27ac) and further sequence motif analysis, provide
67 integrative information about cell identity[9,10].

68 We examined a panel of twenty-five neuroblastoma cell lines (Table S1) and two primary
69 human neural crest cell (hNCC) lines[11]. SEs were defined by the ROSE algorithm[12] modified to
70 account for copy number changes. Principal Component Analysis (PCA), based on scores of SEs
71 identified in at least two neuroblastoma cell lines or in both hNCC lines (n=5975) revealed two
72 distinct groups (Figure 1a): group I with 18 neuroblastoma cell lines and group II comprising the
73 GIMEN, SH-EP and GICAN neuroblastoma cell lines. Group II closely resembled the hNCC
74 lines in this analysis. Four neuroblastoma cell lines occupied an intermediate position between
75 groups I and II. These included the phenotypically heterogeneous SK-N-SH cell line whereas its
76 sub-clones, SH-SY5Y and SH-EP, were included in groups I and II, respectively. This result is
77 consistent with SH-SY5Y cells displaying neurite-like processes and expressing noradrenergic
78 biosynthetic enzymes TH and DBH (“N” phenotype), and SH-EP cells exhibiting a substrate-
79 adherent “S” phenotype without expression of TH and DBH[13]. We also profiled the SE
80 landscape of six patient-derived xenografts (PDXs), five of them with *MYCN* amplification
81 (Table S2). All PDXs clustered with group I when included in the PCA (Figure 1a).

82 SEs were then sorted according to the median H3K27ac signal for each group (Figure 1b
83 and 1c, respectively; Table S3). In group I, the strongest SEs comprise a set of transcription
84 factor (TF) loci including *HAND2*, *PHOX2A*/*PHOX2B* and *GATA2*/*GATA3* and the *ALK*
85 oncogene locus (Figure 1b, 1d, 1e, Figures S1 and S2). These findings are consistent with
86 previous SE data on a few neuroblastoma cell lines[14,15]. PHOX2B, HAND2, and GATA3 are
87 known to participate in a complex TF network controlling normal sympathetic neuron
88 specification and differentiation[16,17]. Recurrent SEs in these TFs therefore appear to be a
89 hallmark of sympathetic cell identity. Most SEs of group II overlapped with SEs of hNCC lines
90 (Figure 1c), consistent with the results of the PCA analysis.

91 Our analysis found *MYCN* SEs for 10 out of 18 cell lines of group I, with or without

92 *MYCN* amplification, and 3 PDX (Figure S3). No groups linked to the *MYCN* or *ALK* status were
93 revealed in the PCA. Furthermore, supervised analysis of SE scores did not indicate SEs
94 associated with *MYCN* amplification or *ALK* mutations (Tables S4 and S5). Cell lines with a
95 *PHOX2B* mutation were observed in group I (SH-SY5Y), group II (SH-EP) or in the
96 intermediate group (SK-N-SH).

97 To detect driver TFs for groups I and II, we used i-cisTarget to find DNA sequence
98 motifs enriched in the SEs with the highest score. For group I, this analysis identified a
99 TAATYYAATTA binding motif common to several homeobox proteins, including PHOX2B
100 and PHOX2A (Figure S4). During sympathetic nervous system development PHOX2B regulates
101 PHOX2A expression[18]. Both TFs are highly expressed in most neuroblastoma cell lines and
102 primary tumors (Figure S5). PHOX2B was undetectable at the transcript and protein level solely
103 in the group II cell lines as well as in the hNCC lines, but was expressed in all other
104 neuroblastoma cell lines (Figure 1f; Figure S6). There was a corresponding lack of SE at
105 *PHOX2B* and no TH and DBH transcription in GIMEN, SH-EP and GICAN (Figure S7). I-
106 cisTarget analysis showed enrichment in AP-1 motif in group II and in the hNCC lines (Figures
107 S8 and S9). AP-1 is a heterodimer composed of FOS and JUN family members both of which are
108 expressed in immature hNCC[11]. These results suggest that PHOX2B participates in the activity
109 of neuroblastoma group I SEs while the AP-1 complex TFs influence the SE landscape of group
110 II.

111 A CRC calling algorithm[9,19] identified PHOX2B as group I-specific CRC TF and FOSL1,
112 FOSL2 and JUN for group II (Figure S10), consistent with our i-cisTarget results. We therefore
113 searched for TFs predicted to be in a CRC either with PHOX2B or a FOS/JUN family member
114 (Figure 1g). Cell lines showing an intermediate position in the PCA had a CRC that included
115 several TFs of both PHOX2B-associated and FOS/JUN-associated sets. Most of TFs of the latter
116 set are expressed in neural crest cells and/or mesenchymal neural crest derivatives. The CRCs of
117 the six PDXs were highly similar to those of the group I cell lines (Figure 1g). As we
118 documented that SE strength linearly correlated with gene expression (Figure S11), we used the
119 latter to further define fully connected TF modules. This analysis revealed two main TF modules
120 distinguishing groups I and II (Figure 1h). PHOX2B, GATA3 and HAND2 were present in
121 module 1 whereas module 2 included FOSL1 and FOSL2. These modules were anti-correlated at
122 the gene expression level. Western blot analysis confirmed the co-expression of several TFs in

123 group I or group II (Figure S12). Furthermore, single cell analysis showed that the SK-N-AS and
124 SK-N-SH cell lines are heterogeneous and comprise cells expressing TFs of either module 1 or
125 module 2 within the same population (Figure 1i, Figure S13, Table S6).

126 Taken together, these data demonstrate a novel type of heterogeneity in neuroblastoma
127 cell lines and suggest that individual cells assume either a sympathetic noradrenergic identity,
128 characterized by a CRC module including PHOX2B, HAND2 and GATA3, and subsequent
129 expression of the enzymes TH and/or DBH; or an NCC-like identity, characterized by expression
130 of a distinct module including FOS and JUN family members but lacking PHOX2B and
131 noradrenergic marker expression. Both types of identity are observed in several heterogeneous
132 cell lines. All cell lines with *MYCN* amplification except one (CHP-212) had a noradrenergic
133 identity whereas cell lines without *MYCN* amplification displayed any of the three identities
134 (Figure 1g).

135 To explore whether the different identity classes seen in neuroblastoma cell lines are also
136 characteristic for neuroblastoma primary tumors, expression data from a large set of primary
137 tumors (n=498; dataset GSE49711)[20] were studied. Correlations between expression of the TFs
138 of each module identified in cell line CRCs were calculated for these primary tumors. We found
139 strong positive correlations between PHOX2B, HAND2, and GATA3 of module 1 as well as
140 between the TFs of the NCC-like module (Figure 2a). We also observed anti-correlations
141 between PHOX2B, HAND2, and GATA3 on the one hand, and TFs of the NCC-like module on
142 the other hand. These results therefore confirm the data obtained with cell lines and further
143 define a PHOX2B/HAND2/GATA3 noradrenergic CRC module in primary neuroblastomas.
144 Next, we used the average expression of the two modules to explore primary tumor identity. All
145 but two tumors showed high expression of the noradrenergic module (Figure 2b). A continuum
146 was observed between low to high values of the NCC-like module, suggesting heterogeneity of
147 cell identity in primary tumors. The remaining two cases with low noradrenergic and high NCC-
148 like module expression may correspond to rare cases with full NCC-like identity, as described
149 for group II cell lines. Similar to the cell lines (Figure S14), lower expression of the NCC-like
150 module was observed in the majority of *MYCN*-amplified tumors (two-sided Wilcoxon signed-
151 rank test p-value 1.01×10^{-10}). A role for MYCN in downregulation of genes from this module is
152 consistent with its promotion of peripheral neuron differentiation from multipotent avian NCC[21].

153 Next, expression of the NCC-like and noradrenergic modules was evaluated in a series of

154 10 diagnosis/relapse sample pairs[22]. Different patterns were observed between the two disease
155 stages (Figure 2c). To address a possible link between heterogeneity of cell identity and
156 treatment response, we investigated the effect of chemotherapy on the NCC-like SH-EP and
157 noradrenergic SH-SY5Y cell lines. SH-EP cells were more resistant to the three agents used
158 (Figure S15). Treatment of the parental SK-N-SH cell line with doxorubicin or cisplatin resulted
159 in the respective decreased or increased expression of module 1 and 2 (Figure 2d). Enrichment of
160 cells with an NCC-like identity thus correlates with better drug resistance. However, we cannot
161 exclude that treatment may also induce transdifferentiation from noradrenergic to NCC-like
162 identity. The observation that tumors at relapse are not systematically enriched in NCC-like cells
163 supports the concept of plasticity in the reversion of cell identity. This may rely on a switch from
164 adrenergic to NCC-like identity under chemotherapy and from NCC-like to noradrenergic after
165 treatment. Altogether, these data underline the importance of targeting both types of cells during
166 treatment.

167 Strong correlations between PHOX2B, HAND2 and GATA3 expression were observed
168 both in cell lines and tumors. Phox2b directly binds Hand2 protein[23], and Phox2b, Hand2 and
169 Gata3 cross-regulate during sympathetic nervous system development[16]. We therefore performed
170 ChIP-seq analysis for these TFs in the CLB-GA neuroblastoma cell line and identified binding
171 motifs for PHOX2B, HAND2 (zinc finger TF) and GATA3 (bHLH leucine zipper TF) (Figure
172 3a). Binding regions for all three TFs corresponded to the H3K27ac peaks in the *PHOX2B*,
173 *GATA3*, *HAND2* and *ALK* SEs and also in the *MYCN* SE (Figure 3b and 3c, Figure S16). These
174 results therefore confirm the biological existence of the noradrenergic module, showing that
175 PHOX2B, HAND2 and GATA3 are SE-regulated and bind to the SEs of each other (Figure 3d).
176 We next investigated the occupancy by these TFs of 4,336 SE regions predicted in at least two
177 neuroblastoma cell lines. SE regions were ranked according to average SE score and intersection
178 with TF binding sites was evaluated. Over 90% of the strong and recurrent neuroblastoma SEs
179 were co-occupied by PHOX2B, HAND2 and GATA3 (Figure 3e). Additionally, positional
180 binding analysis showed that HAND2, PHOX2B and GATA3 bind the same ~400 bp-long
181 regions within active regulatory regions (Figure 3f). Altogether, our results demonstrate that
182 PHOX2B, HAND2 and GATA3 are master TFs defining the SE landscape of neuroblastoma cell
183 lines with a noradrenergic identity.

184 It has been demonstrated that cancer dependencies can be found among SE-marked

185 genes[19,24]. Although missense and frameshift *PHOX2B* mutations predispose to
186 neuroblastoma[25,26], its role in sporadic neuroblastoma remains poorly understood. Phox2b knock-
187 out mice completely lack autonomic structures[17] whereas conditional knock-out leads to
188 decreased neuroblast proliferation[27]. An effect of PHOX2B knockdown on neuroblastoma cell
189 proliferation has been previously suggested[28]. To further document the consequence of PHOX2B
190 knockdown on neuroblastoma growth, we generated a doxycycline-inducible anti-*PHOX2B*
191 short-hairpin RNA (shRNA) expression system in noradrenergic CLB-GA and SH-SY5Y cells.
192 Inducible decrease of PHOX2B protein (Figure 4a, 4c) resulted in significant inhibition of
193 neuroblastoma cell growth (Figure 4b, 4d, Figure S17). Decreased expression of PHOX2B in
194 CLB-GA cells also impaired tumor growth *in vivo* (Figure 4e and 4f, Figure S18). We then
195 evaluated whether PHOX2B decrease was sufficient to change the noradrenergic identity of the
196 CLB-GA and SH-SY5Y cell lines to an NCC-like identity. However, data obtained by RNA-seq
197 and RT-q-PCR suggested that the residual level of PHOX2B was sufficient to maintain a
198 noradrenergic identity (Figure S19). This observation is consistent with the noradrenergic
199 identity of the CLB-PE cell line in which PHOX2B expression is low but detected at the protein
200 and RNA levels (Figures 1f and S6).

201 We observed a reduction of proliferation upon HAND2 and GATA3 knockdown in
202 several cell lines, consistently with previous data on GATA3 knockdown[15] (Figure S20). These
203 results are in line with Hand2 and Gata3 controlling sympathetic neuroblast proliferation[16].
204 Neuroblastoma cells of noradrenergic identity therefore appear to be addicted to these key
205 lineage TFs as well as to PHOX2B[29].

206 In conclusion, our work provides fundamental insights into the transcriptomic and
207 epigenomic landscape of neuroblastoma. Distinct TF networks predicate different tumor
208 identities, corresponding to sympathetic noradrenergic or NCC-like identity. Most primary
209 tumors comprise cells of both identities, revealing a novel aspect of tumor heterogeneity.
210 Neuroblastoma treatment should benefit from specifically targeting both identities.

211
212
213
214

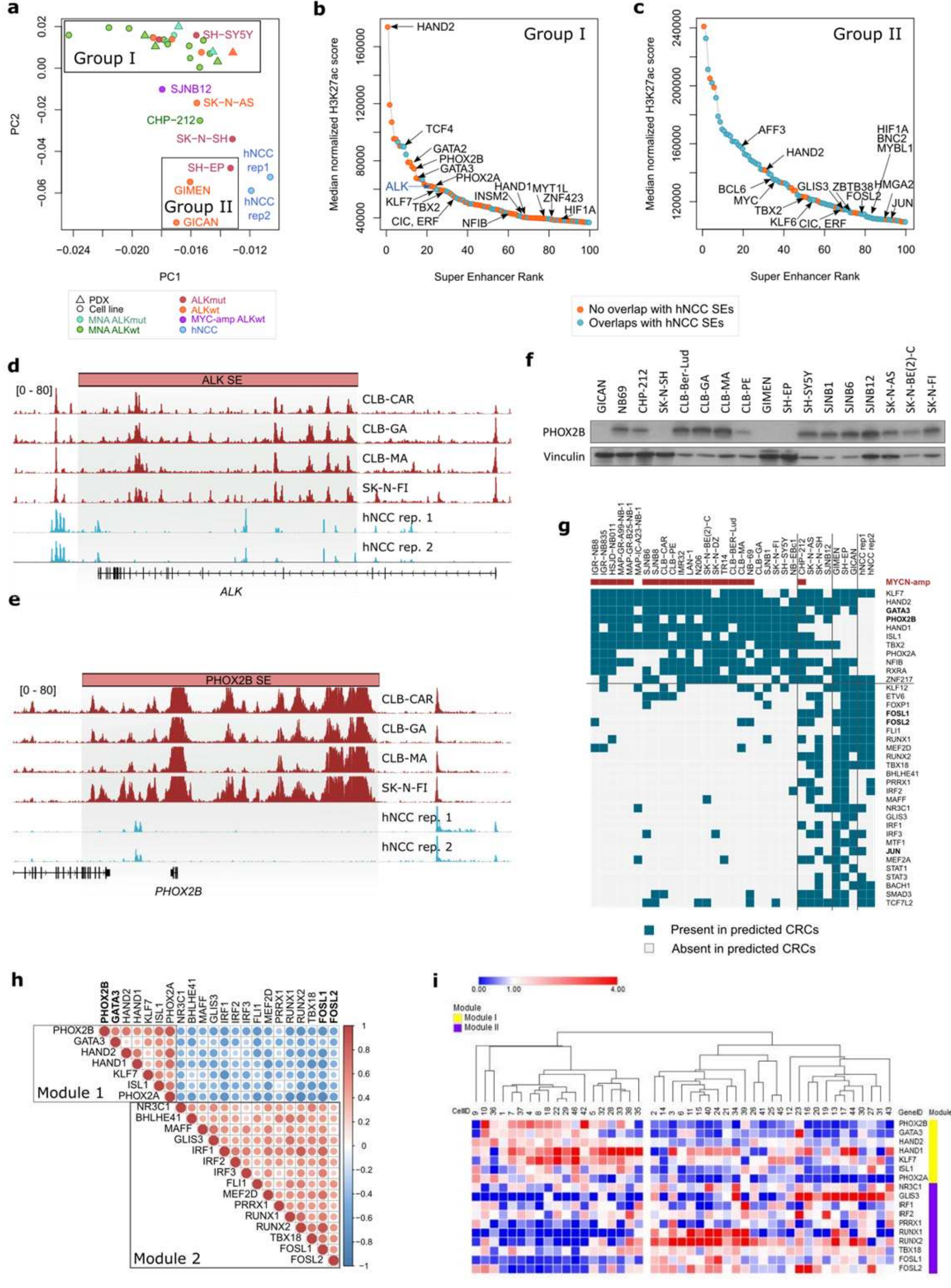
a
Group I
SH-SY5Y
SJNB12
SK-N-AS
CHP-212
SK-N-SH
SH-EP
GIMEN
Group II
GICAN
hNCC rep1
hNCC rep2
PC1
PC2
PDX
Cell line
MNA ALKmut
MNA ALKwt
ALKmut
ALKwt
MYC-amp ALKwt
hNCC
b
Group I
Median normalized H3K27ac score
Super Enhancer Rank
HAND2
TCF4
GATA2
PHOX2B
GATA3
PHOX2A
ALK
KLF7
TBX2
CIC, ERF
HAND1
INSM2
MYT1L
ZNF423
HIF1A
NFIB
c
Group II
AFF3
HAND2
BCL6
MYC
TBX2
GLIS3
ZBTB38
FOSL2
HMGA2
JUN
KLF6
CIC, ERF
HIF1A
BNC2
MYBL1
No overlap with hNCC SEs
Overlaps with hNCC SEs
d
ALK SE
[0 - 80]
CLB-CAR
CLB-GA
CLB-MA
SK-N-FI
hNCC rep. 1
hNCC rep. 2
ALK
e
PHOX2B SE
[0 - 80]
CLB-CAR
CLB-GA
CLB-MA
SK-N-FI
hNCC rep. 1
hNCC rep. 2
PHOX2B
f
GICAN
NB69
CHP-212
SK-N-SH
CLB-Ber-Lud
CLB-GA
CLB-MA
CLB-PE
GIMEN
SH-EP
SH-SY5Y
SJNB1
SJNB6
SJNB12
SK-N-AS
SK-N-BE(2)-C
SK-N-FI
PHOX2B
Vinculin
g
MYCN-amp
KLF7
HAND2
GATA3
PHOX2B
HAND1
ISL1
TBX2
PHOX2A
NFIB
RXRA
ZNF217
KLF12
ETV6
FOXP1
FOSL1
FOSL2
FLI1
RUNX1
MEF2D
RUNX2
TBX18
BHLHE41
PRRX1
IRF2
MAFF
NR3C1
GLIS3
IRF1
IRF3
MTF1
JUN
MEF2A
STAT1
STAT3
BACH1
SMAD3
TCF7L2
Present in predicted CRCs
Absent in predicted CRCs
h
Module 1
Module 2
PHOX2B
GATA3
HAND2
HAND1
KLF7
ISL1
PHOX2A
NR3C1
BHLHE41
MAFF
GLIS3
IRF1
IRF2
IRF3
FLI1
MEF2D
PRRX1
RUNX1
RUNX2
TBX18
FOSL1
FOSL2
i
0.00
1.00
4.00
Module
Module I
Module II
CellID
GeneID

216 **Figure 1. SE landscape reveals various CRCs and identities in neuroblastoma cell lines. a**,
217 Principal Component Analysis (PCA) based on neuroblastoma and hNCC SE log scores. MNA:
218 MYCN amplification. **b, c**, Ranked plot for the 100 SEs with the highest median H3K27ac score
219 in neuroblastoma cell line groups I and II, respectively. TFs are indicated in black with arrows.
220 **d, e,** Tracks for ChIP-seq profiles for H3K27ac binding at *ALK* and *PHOX2B* SEs, respectively.
221 **f**, Western blot analysis of PHOX2B and vinculin as a loading control in a panel of
222 neuroblastoma cell lines. SK-N-SH cells correspond to batch 1. **g**, TFs predicted to participate in
223 a CRC with PHOX2B (upper part) or with a FOS/JUN family member (lower part) in
224 neuroblastoma cell lines. TFs whose binding motifs are enriched in SEs of group I and II are
225 shown in bold. **h**, Pearson correlation matrix for the expression values of 22 TFs identified in
226 CRCs of cell lines shows strong positive correlations within module 1 and module 2; correlation
227 is calculated for RNA-seq data in neuroblastoma cell lines and PDX (n=31). **i**, Single cell
228 analysis reveals heterogeneity of cell identity in the SK-N-AS cell line. Expression of TF of
229 modules 1 and 2 was evaluated by RT-q-PCR and data were normalized to the SK-N-AS cell
230 population overall.
231
232
233
234
235
236

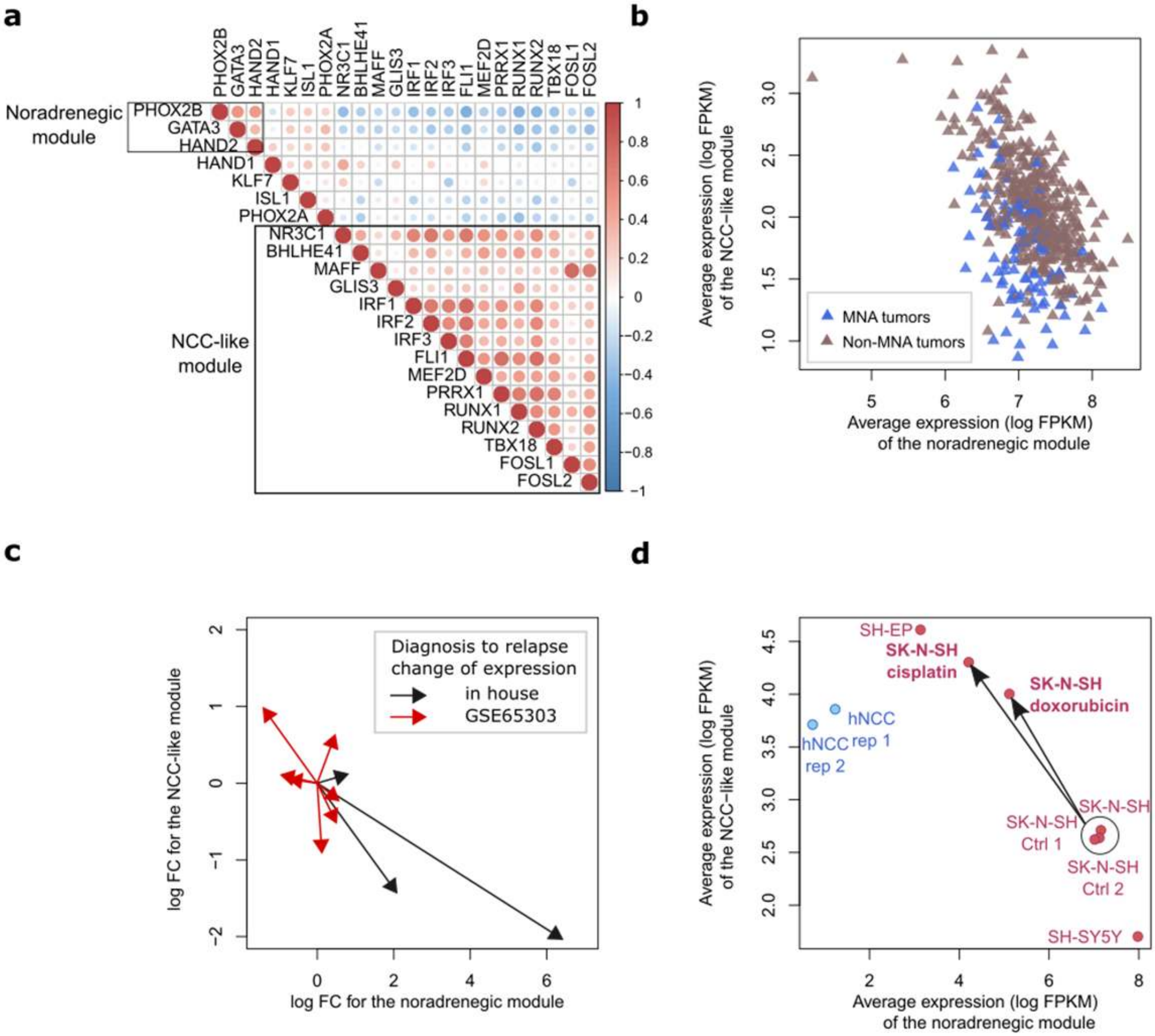

237

238 **Figure 2. Different identity of neuroblastoma primary tumors and impact of chemotherapy**
239 **on cell identity**. **a**, Pearson correlation matrix for the 22 TFs identified in CRCs of cell lines in a
240 set of 498 neuroblastoma primary tumors. **b,** Mean expressions of the noradrenergic and NCC-
241 like modules negatively correlate in the whole set of tumors (Pearson R = -0.49, one-sided
242 permutation test p-value < 10^{-10}) and define a continuum between full noradrenergic and NCC-
243 like cases. Blue: tumors with *MYCN* amplification. **c**, Identity of tumor pairs at diagnosis and
244 relapse revealed by expression profiling. The series includes 7 pairs from the GSE65303
245 dataset[22] (red) and 3 in-house pairs (black). **d**, Treatment of SK-N-SH cells with chemotherapy
246 favors cells with an NCC-like identity. Cells used in this experiment (batch 2) were more
247 noradrenergic compared to the ones used in the ChIP-seq experiment (batch 1).

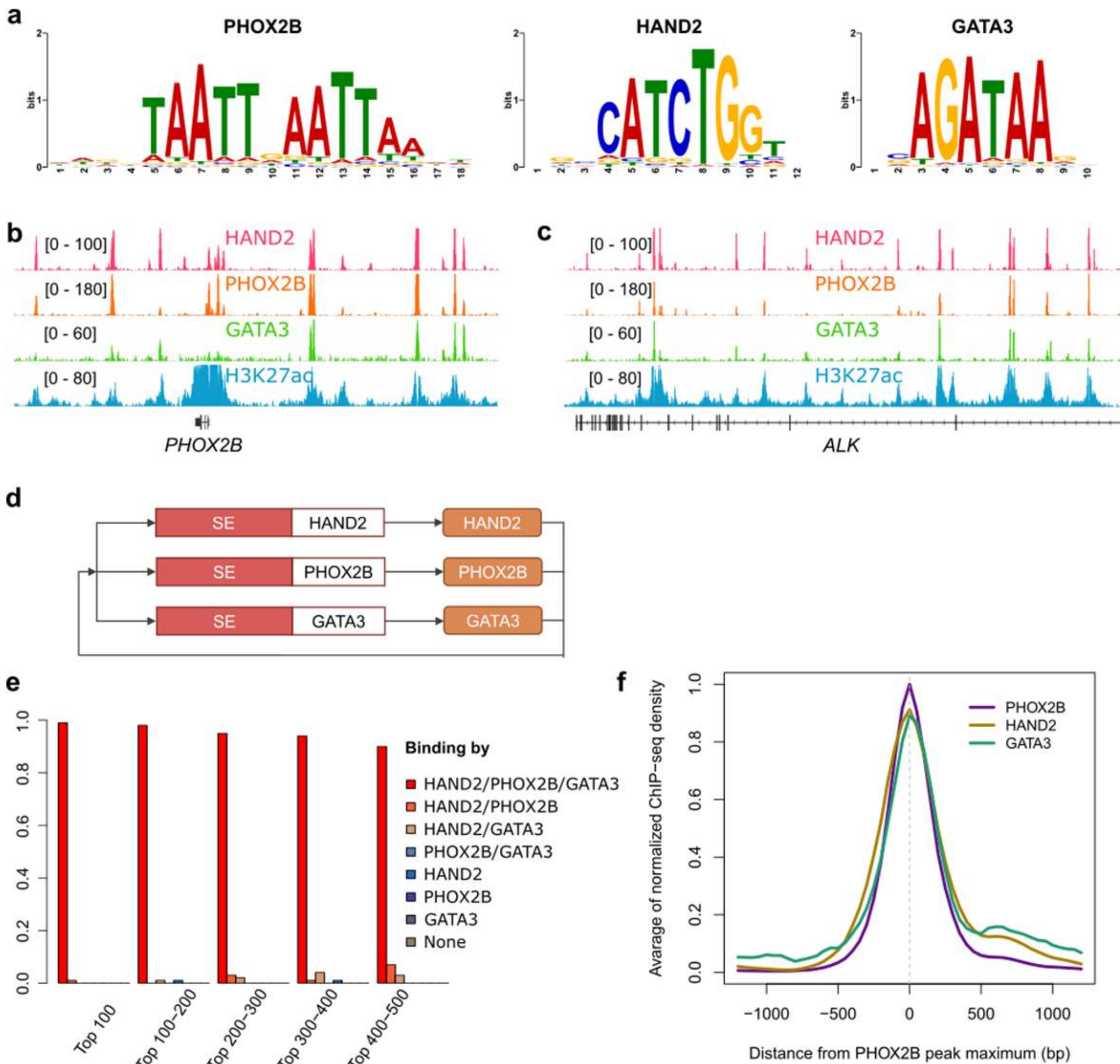

248

249 **Figure 3. PHOX2B, HAND2 and GATA3 are master transcription factors defining the SE**
250 **landscape of noradrenergic neuroblastoma. a**, *De novo* identification of PHOX2B, HAND2
251 and GATA3 TF binding motifs. **b** and **c**, Tracks for ChIP-seq profiles for PHOX2B, HAND2,
252 GATA3 and H3K27ac binding at *PHOX2B* and *ALK* SEs, respectively. **d**, CRC of activating TFs
253 that define a noradrenergic module. **e**, Neuroblastoma SEs defined by H3K27ac peaks are
254 simultaneously occupied by PHOX2B, HAND2 and GATA3. **f**, HAND2, PHOX2B and GATA3
255 bind closely located regions within neuroblastoma SEs (summary of densities of 2,078 binding
256 sites corresponding to 500 top neuroblastoma SEs).

257

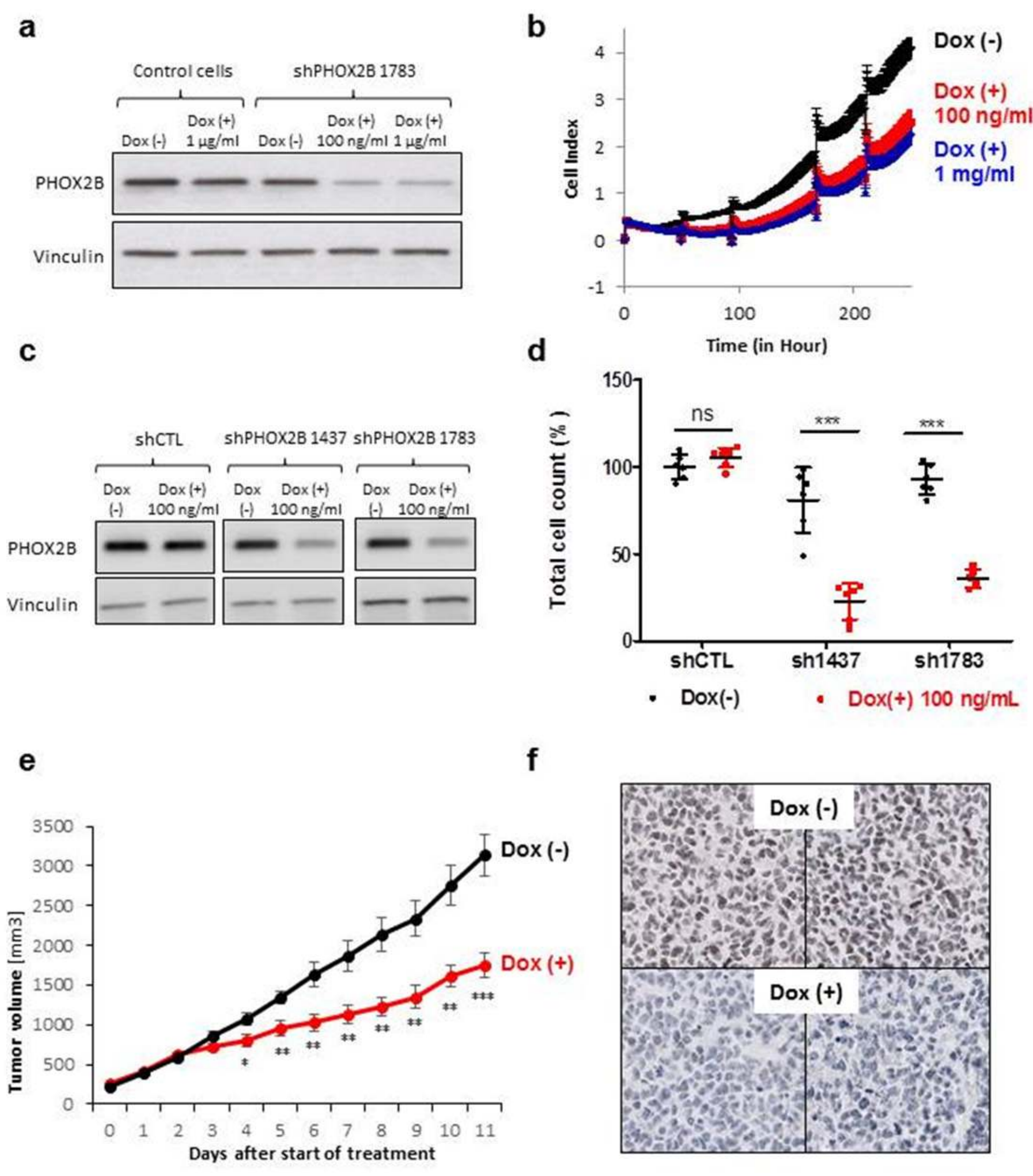

258

259

260 **Figure 4. PHOX2B is critical for the growth of noradrenergic neuroblastoma cells. a**,
261 PHOX2B knockdown following doxycycline treatment was confirmed at 72 h by immunoblot
262 (loading control: vinculin) in CLB-GA neuroblastoma cells infected with a shRNA targeting
263 *PHOX2B* vector. **b**, xCELLigence^{TM} proliferation kinetics of infected CLB-GA cells in absence

264 or presence of doxycycline at 100 ng/ml or 1 µg/ml. Data shown are the mean ± s.d. of results
265 obtained in the different conditions (n=5 technical replicates). **c**, PHOX2B immunoblot of SH-
266 SY5Y neuroblastoma cells infected with 2 different shRNA vectors targeting *PHOX2B,* at 72 h.
267 **d**, Cell counts for the SH-SY5Y cell line infected with sh1437 or sh1783 vectors targeting
268 PHOX2B or with the control shCTL vector. 10^5 cells were plated in 24-well plates at day 0 in the
269 absence or presence of doxycycline at 100 ng/ml. The number of living cells was counted at day
270 8 (Mean ± s.d.; n=6 replicates). **e**, Growth curves for subcutaneously xenografted sh1783
271 transduced CLB-GA cells. When tumors reached a volume of around 170 mm3, doxycycline and
272 sucrose (Dox +) or sucrose alone (Dox −) was added to the drinking water (Mean ± s.e.m.; n =8
273 mice per group). P values were determined via two-tailed unpaired Welch's t-test (***:
274 p<0.001). **f**, PHOX2B immunohistochemistry (brown) combined with Hematoxylin staining in
275 two xenografts treated with doxycycline and two control xenografts.

276

277

278

279

280

281

282

283

284

285

286

287

288 **References**

289 1. Matthay, K. K. *et al.* Neuroblastoma. *Nat. Rev. Dis. Primer* **2,** 16078 (2016).
290 2. Brodeur, G. M., Seeger, R. C., Schwab, M., Varmus, H. E. & Bishop, J. M. Amplification
291 of N-myc in untreated human neuroblastomas correlates with advanced disease stage. *Science*
292 **224,** 1121–4 (1984).
293 3. Mosse, Y. P. *et al.* Identification of ALK as a major familial neuroblastoma
294 predisposition gene. *Nature* **455,** 930–5 (2008).
295 4. Janoueix-Lerosey, I. *et al.* Somatic and germline activating mutations of the ALK kinase
296 receptor in neuroblastoma. *Nature* **455,** 967–70 (2008).
297 5. George, R. E. *et al.* Activating mutations in ALK provide a therapeutic target in
298 neuroblastoma. *Nature* **455,** 975–8 (2008).
299 6. Chen, Y. *et al.* Oncogenic mutations of ALK kinase in neuroblastoma. *Nature* **455,** 971–4
300 (2008).
301 7. Peifer, M. *et al.* Telomerase activation by genomic rearrangements in high-risk
302 neuroblastoma. *Nature* **526,** 700–704 (2015).
303 8. Valentijn, L. J. *et al.* TERT rearrangements are frequent in neuroblastoma and identify
304 aggressive tumors. *Nat. Genet.* **47,** 1411–1414 (2015).
305 9. Saint-André, V. *et al.* Models of human core transcriptional regulatory circuitries.
306 *Genome Res.* **26,** 385–396 (2016).
307 10. Hnisz, D. *et al.* Super-enhancers in the control of cell identity and disease. *Cell* **155,** 934–
308 947 (2013).
309 11. Thomas, S. *et al.* Human neural crest cells display molecular and phenotypic hallmarks of
310 stem cells. *Hum Mol Genet* **17,** 3411–25 (2008).
311 12. Whyte, W. A. *et al.* Master transcription factors and mediator establish super-enhancers
312 at key cell identity genes. *Cell* **153,** 307–319 (2013).
313 13. Ross, R. A., Spengler, B. A. & Biedler, J. L. Coordinate morphological and biochemical
314 interconversion of human neuroblastoma cells. *J. Natl. Cancer Inst.* **71,** 741–747 (1983).
315 14. Chipumuro, E. *et al*. CDK7 Inhibition Suppresses Super-Enhancer-Linked Oncogenic
316 Transcription in MYCN-Driven Cancer. *Cell* **159**, 1126-1139 (2014).
317 15. Oldridge, D. A. *et al*. Genetic predisposition to neuroblastoma mediated by a LMO1
318 super-enhancer polymorphism. *Nature* **528**, 418-421 (2015).

319 16. Rohrer, H. Transcriptional control of differentiation and neurogenesis in autonomic
320 ganglia. *Eur J Neurosci* **34,** 1563–73 (2011).
321 17. Pattyn, A., Morin, X., Cremer, H., Goridis, C. & Brunet, J. F. The homeobox gene
322 Phox2b is essential for the development of autonomic neural crest derivatives. *Nature* **399,** 366–
323 70 (1999).
324 18. Flora, A. *et al.* Sp proteins and Phox2b regulate the expression of the human Phox2a
325 gene. *J. Neurosci.* **21,** 7037–7045 (2001).
326 19. Lin, C. Y. *et al.* Active medulloblastoma enhancers reveal subgroup-specific cellular
327 origins. *Nature* **530,** 57–62 (2016).
328 20. Zhang, W. *et al.* Comparison of RNA-seq and microarray-based models for clinical
329 endpoint prediction. *Genome Biol.* **16,** (2015).
330 21. Wakamatsu, Y., Watanabe, Y., Nakamura, H. & Kondoh, H. Regulation of the neural
331 crest cell fate by N-myc: promotion of ventral migration and neuronal differentiation.
332 *Development* **124,** 1953–62 (1997).
333 22. Schramm, A. *et al.* Mutational dynamics between primary and relapse neuroblastomas.
334 *Nat. Genet.* **47,** 872–877 (2015).
335 23. Reiff, T. *et al.* Neuroblastoma phox2b variants stimulate proliferation and
336 dedifferentiation of immature sympathetic neurons. *J. Neurosci.* **30,** 905–915 (2010).
337 24. Chapuy, B. *et al.* Discovery and characterization of super-enhancer-associated
338 dependencies in diffuse large B cell lymphoma. *Cancer Cell* **24,** 777–790 (2013).
339 25. Trochet, D. *et al.* Germline mutations of the paired-like homeobox 2B (PHOX2B) gene
340 in neuroblastoma. *Am J Hum Genet* **74,** 761–4 (2004).
341 26. Mosse, Y. P. *et al.* Germline PHOX2B mutation in hereditary neuroblastoma. *Am J Hum*
342 *Genet* **75,** 727–30 (2004).
343 27. Coppola, E., d'Autréaux, F., Rijli, F. M. & Brunet, J.-F. Ongoing roles of Phox2
344 homeodomain transcription factors during neuronal differentiation. *Development* **137,** 4211–
345 4220 (2010).
346 28. Ke, X.-X. *et al.* Phox2B correlates with MYCN and is a prognostic marker for
347 neuroblastoma development. *Oncol. Lett.* **9,** 2507–2514 (2015).
348 29. Garraway, L. A. & Sellers, W. R. Lineage dependency and lineage-survival oncogenes in
349 human cancer. *Nat. Rev. Cancer* **6,** 593–602 (2006).

350 # Online Methods

351

352 **Neuroblastoma and hNCC cell lines**

353

354 Neuroblastoma cell lines used in this study have been previously described[30]. CHP-212, IMR-32,
355 SH-SY5Y, SK-N-AS, SK-N-BE(2)C, SK-N-DZ, SK-NF-I and SK-N-SH were obtained from the
356 American Type Culture Collection (ATCC). CLB cell lines were derived by V. Combaret (Lyon,
357 France). The SH-EP and LAN-1 cell lines have been kindly provided by M. Schwab
358 (Heidelberg, Germany) and J. Couturier (Paris, France). Lines GIMEN, N206, SJNB1, SJNB6,
359 SJNB8, SJNB12 and TR-14 were obtained from R. Versteeg (Amsterdam, The Netherlands) and
360 line GICAN was a kind gift from M. Ponzoni (Genova, Italy). The NB69 and NB-EBc1 cell lines
361 were obtained from the European Collection of Authentified Cell Cultures and from the
362 Children's Oncology Group, respectively. A first batch of SK-N-SH cells (batch 1) was used for
363 the ChIP-seq and single cell analysis. A second batch (batch 2) was used for the evaluation of the
364 chemotherapeutic agents. Batch 2 was enriched in adrenergic cells. Cell line authentication was
365 performed by comparison of the genomic copy number profile calculated from the input ChIP-
366 seq data obtained using Control-FREEC[31] (see below) with SNP array profile and STR profiling
367 for ATCC cell lines. Cells were checked routinely by PCR for the absence of mycoplasma.
368 Neuroblastoma cell lines were cultured at 37°C with 5% CO_2 in a humidified atmosphere in
369 RPMI (GE Healthcare, for CLB cell lines, SH-EP, GICAN and NB69), in IMDM (Gibco) for
370 NB-EBc1 (according to the provided conditions) or DMEM (GE Healthcare, for other cell lines),
371 with 10%, 15% or 20% FCS (Eurobio) and 100 µg/ml penicillin/streptomycin (Gibco). Primary
372 hNCC lines were grown as previously described[32] under bioethical approval PFS14-011 from the
373 French Biomedical Agency for the use of human embryonic material to S. Zaffran. Briefly, cells
374 were grown in Glutamax DMEM:F12 [Gibco] supplemented with 12% FCS (Eurobio), 100
375 µg/ml penicillin/streptomycin, 10 mM HEPES, 100 ng/ml hydrocortisone, 10 µg/ml transferrin,
376 400 pg/ml 3,3,5-thio-iodo-thyronine, 10 pg/ml glucagon, 100 pg/ml epidermal growth factor, 1
377 ng/ml insulin and 200 pg/ml fibroblast growth factor 2 (all products supplied by Sigma-Aldrich
378 except EGF and FGF2 from Gibco).

379

380

381 **PDX models**

382

383 Neuroblastoma PDXs were obtained from stage L2 (MAP-IC-A23-NB-1), stage 3 (IGR-NB8) or
384 stage 4 (IGR-N835, MAP-GR-A99-NB-1, MAP-GR-B25-NB-1 and HSJD-NB-011[33]). None of
385 them was related to the used cell lines. All PDXs but MAP-IC-A23-NB-1 had *MYCN*
386 amplification. PDXs IGR-NB8, IGR-N835[34,35] were obtained using female Swiss nude mice of
387 6-8 weeks at engraftment whereas female NSG mice were used for MAP-GR-A99-NB-1 and
388 MAP-GR-B25 PDXs. These PDX models are developed and maintained within the project
389 "Development of Pediatric PDX models" approved by the experimental ethic committee 26
390 (CEEA26 – Gustave Roussy) under the number 2015032614359689v7. The MAP-IC-A23-NB-1
391 (IC-pPDX-17) and HSJD-NB-011 models were obtained using female SCID mice of 10-11
392 weeks or female Swiss nude mice of 3-6 weeks at engraftment. Animal studies at SJD were
393 approved by the local animal care and use committee (Comite Etico de Experimentacion Animal
394 at Universidad de Barcelona, protocol 135/11). All experiments were performed in accordance
395 with European legislation. MAP-IC-A23-NB-1, MAP-GR-A99-NB-1 and MAP-GR-B25-NB-1
396 PDXs were obtained through the Mappyacts protocol (clinicaltrial.gov: NCT02613962).

397

398 **Patient samples**

399

400 Three diagnosis/relapse pairs of tumors (Pair1/2/3-Diagnosis and Relapse; all stage 4; Table S2)
401 were studied in this work. The relapse samples were obtained through the Mappyacts protocol.
402 The MAP-GR-B25-NB-1 PDX was derived from the relapse of pair 1. Analysis of biological
403 material from patients, including study of expression profiles of neuroblastoma samples was
404 approved by the Institut Curie's Institutional Review Board. This study was authorized by the
405 decision of the ethics committees « Comité de Protection des Personnes Sud-Est IV », references
406 L07–95 and L12–171, "Comité de Protection des Personnes Ile de France 1", reference 0811728
407 and "Comité de Protection des Personnes Ile de France 3" reference 3272. Written informed
408 consent was obtained from parents or guardians according to national law.

409

410

411

412 **ChIP-sequencing**

413

414 H3K27ac, PHOX2B, HAND2 and GATA3 chromatin immunoprecipitation (ChIP) was
415 performed using the iDeal ChIP-seq kit for Histones or iDeal ChIP-seq kit for Transcription
416 Factors (Diagenode) using the following antibodies: ab4729 (rabbit polyclonal, Abcam) for
417 H3K27ac, sc-376997X (mouse monoclonal), sc-9409 and sc-22206X (goat polyclonal) from
418 Santa Cruz Biotechnology for PHOX2B, HAND2 and GATA3, respectively. Ten million cells
419 were cross-linked with 1% formaldehyde for 10 min followed by quenching with 125 mM
420 glycine final concentration for 5 min at room temperature. Chromatin was isolated by the
421 addition of lysis buffer, and lysates sonicated to obtain sheared chromatin to an average length of
422 ~ 300 bp. ChIP was performed with chromatin of 1 million cells for H3K27ac and 3.75 million
423 cells for transcription factors. The equivalent of 1% of chromatin used for TFs was kept to
424 quantify input and reverse cross-linked 4h at 65°C with proteinase K. ChIP was performed
425 overnight at 4°C on a rotating wheel with 1 µg of antibody for H3K27ac, 2 µg for HAND2 and 5
426 µg for PHOX2B and GATA3. Protein A-coated magnetic beads were precleared with antibodies
427 3h at 4°C only for transcription factors. After ChIP, chromatin was eluted 30 min at room
428 temperature and reverse cross-linked 4h at 65°C with proteinase K. DNA was precipitated and
429 purified with magnetic beads with the Ipure kit (Diagenode). Before sequencing, ChIP efficiency
430 was validated by quantitative PCR for each antibody on specific genomic regions using
431 powerSYBR® Green Master mix (Applied Biosystems) and compared for each primer pair to the
432 input DNA. Primers are available upon request.
433 For PDX samples, frozen tumors were reduced to powder with a pestle and then resuspended in
434 PBS. Crosslinking of chromatin was performed by adding 1% formaldehyde for 8 min with
435 agitation on a rotating wheel. Lysis of cells, fragmentation of chromatin and ChIP were
436 performed as described above for cell lines using the iDeal ChIP-seq kit for Histones.
437 Illumina sequencing libraries were prepared from ChIP and input DNA using the TruSeq ChIP
438 library preparation kit according to the manufacturer's protocol. Briefly, DNA were subjected to
439 consecutive steps of end-repair, dA-tailing and ligation to TruSeq indexed Illumina adapters.
440 Size-selection was performed only for the H3K27ac ChIP (100 – 600 bp). After a final
441 amplification step of 14 cycles, the resulting DNA libraries were quantified using a qPCR
442 method (KAPA library quantification kit) and sequenced on the Illumina HiSeq2500 instrument

443 (rapid run mode; single reads 100 nts).
444
445 **ChIP-seq analysis**
446
447 ChIP-seq reads were mapped to the human reference genome hg19/GRCh37 using Bowtie2
448 v2.1.0[36]. Low mapping quality reads (Q<20) were discarded; duplicate reads were kept in order
449 to detect signal in genomic amplification regions. Enriched regions (peaks) were called using
450 HMCan v1.30[37] with the following parameters: min fragment length 100 bp, median fragment
451 length 250 bp, maximal fragment length 400 bp, small bin length 50 bp, large bin length 25 kb,
452 p-value threshold 0.05, merging distance 200 bp, number of iterations 20, final threshold 0.1,
453 removing duplicates: False. Regions from the hg19 ENCODE blacklist[38] were excluded from the
454 analysis. HMCan output included ChIP density profiles corrected for the GC-content and copy
455 number bias (*.wig) and narrow and large enrichment regions further called peaks (*.bed).
456 Density profiles were then normalized between samples with an in-house R script based on the
457 median density values in the 5,000 highest peaks discounting the first 100 peaks as they may
458 correspond to amplification regions. Peaks with low signal (i.e., low HMCan score values) were
459 discarded (in-house script correlating peak length and peak signal,
460 https://github.com/BoevaLab/LILY/).
461 The Control-FREEC[31] algorithm was applied to input samples (default parameters; input: *.bam
462 files) to obtain copy number profiles of each cell line. These profiles matched known copy
463 number profiles for these neuroblastoma cell lines.
464 To call enhancers and super-enhancers, a modified version of ROSE[12,39] dubbed LILY was used
465 (http://BoevaLab.com/LILY/). First, large H3K27ac peaks were stitched together, using a default
466 distance of 12.5 kb, while promoter regions (± 2.5 Kb from the transcription start site) were
467 excluded. Then each region received a SE score corresponding to the sum of normalized
468 H3K27ac density values (already corrected for copy number and GC-content bias by HMCan[37]).
469 The regions were sorted according to the SE score. The threshold of the score distinguishing
470 typical enhancers from SEs was determined by ROSE. For twenty-five neuroblastoma cell lines,
471 the average number of SEs identified per cell line was 1,252 (standard deviation 385). The
472 highest number of SEs was detected in GIMEN and SH-EP (1,901 and 1,819 regions
473 respectively).

474 ChIP-seq experiments for H3K27ac were performed once for every sample except for the CLB-
475 GA cell line for which the experiment was performed in two biological replicates. We used these
476 replicate samples to document the reproducibility of the SE calling and SE score calculation
477 (Figure S21). Among the top 500 SEs of replicate 1, 93% were annotated as active SEs in
478 replicate 2.
479 To generate a list of neuroblastoma SEs, we superimposed the SE regions predicted in the
480 twenty-five cell lines and excluded regions shorter than 12 Kb. In order to avoid stitching of
481 several neighboring SE regions into one, long regions with several sub-peaks were separated in
482 sub-regions using as a threshold one half of the median number of SEs. Overall, 4,336 regions
483 with overlapping SEs detected in more than one sample were annotated as putative
484 neuroblastoma SEs (Table S3). SEs were assigned to the RefSeq genes (hg19, version Sep 16,
485 2016) using the information about locations of topologically associating domains (TADs) in
486 eight human cell lines[40]. Among all genes located in the same TAD with a SE and therefore
487 possibly regulated by a SE, we selected these with the highest correlation between the gene
488 expression and the SE score in the 33 samples of these study (threshold 0.361 corresponding to
489 the adjusted p-value ('FDR') of 0.05, Figure S11). Of note, each gene can have several SE
490 regions and each SE can be assigned to a number of genes (Table S3). In total, neuroblastoma
491 SEs were assigned to 4,791 genes. Similarly, we detected and assigned to genes 1,639 SEs active
492 in both hNCC samples.
493 For further analysis, we kept only SE regions active in at least two neuroblastoma cell lines or
494 hNCC samples (5,975 regions). This was done to remove cell-line specific events and false
495 positive predictions of SE regions.
496 Principal Component Analysis (PCA) for 33 samples (25 neuroblastoma cell lines, 6
497 neuroblastoma PDXs and 2 hNCC lines) was performed on log2 values of SE scores of 5,975
498 SEs. Table S3 shows contributions of the SE regions to the first two principal components.
499 Analysis of samples in the first principal components suggested their separation into group I
500 (CLB-GA, CLB-MA, CLB-CAR, CLB-BER-Lud, CLB-PE, NB69, NB-EBc1, SJNB1, SJNB6,
501 SJNB8, IMR-32, LAN-1, N206, SK-N-BE(2)C, SK-N-DZ, SK-N-FI, TR14, SH-SY5Y), group II
502 (GICAN, SH-EP, GIMEN) and the intermediate group (SK-N-SH, SK-N-AS, SJNB12, CHP-
503 212). Table S3 includes information about fold changes and p-values for the two-sided Wilcoxon
504 test for differential analysis of SE scores between group I and II.

505 To detect known transcription factor binding motifs enriched in neuroblastoma SEs (cell lines of
506 group I and II) and SEs of hNCC, we applied the i-cisTarget[41] method to the list of 2,227, 1,850
507 and 1,640 valley regions in H3K27ac peaks overlapping the 100 top SEs of group I and II and
508 hNCC, respectively.
509 CRC in the neuroblastoma cell lines, PDX samples and hNCC lines were detected using
510 COLTRON[19] based on the list of samples' SEs with the following properties: (i) SE score
511 correlated with gene expression in our set of 31 NB samples and (2) SE region was detected in
512 more than 2 cell lines in our study. We then parsed the files with ranked cliques to see whether a
513 given TF was predicted to be involved in a CRC of a given sample. We kept TFs present in over
514 50% of cell lines from group I (n=18) or group II (n=3). This resulted in 69 TFs. From the
515 COLTRON predictions, we excluded 17 transcription factors that were not associated with a SE
516 in our analysis (Figure S10). As motif enrichment analysis discovered a significant enrichment in
517 homeobox and AP-1 motifs of neuroblastoma SEs (Figures S4 and S8), among these 52 TFs, we
518 selected those that were predicted by COLTRON to occur in the same CRC as the homeobox TF
519 PHOX2B or AP-1 TFs (JUN, JUNB, FOSL1 or FOSL2) in more than 50% of cell lines of group
520 I or II. This resulted in 37 TFs (Figure 1g). Clustering of the 37 genes (hclust, McQuitty method)
521 based on the correlation of their expression defined two modules (module 1, n = 7, includes
522 PHOX2B; module 2, n=15, includes FOSL1 and FOSL2) (Figure S22).
523 Motif discovery in ChIP-seq peaks of GATA3, HAND2 and PHOX2B was performed using the
524 Position Analysis tool of the RSAT package[42] (Oligonucleotide size: HAND2: 5; GATA3: 5;
525 PHOX2B: 8).
526 To calculate average ChIP-seq density profiles around the PHOX2B peak maximum positions,
527 we first extracted all 2,400 bp regions centered on PHOX2B ChIP-seq binding sites and kept
528 those that overlapped peaks of all three TFs. We obtained 14,693 such regions throughout the
529 whole human genome for the CLB-GA cell line. 2,078 out of them were located within the 500
530 strongest neuroblastoma SEs. ChIP-seq density for each TF for each region was rescaled to have
531 a maximum value of 1 corresponding to the peak maximum. We then plotted the average
532 rescaled density for the 2,078 regions.
533

534 **RNA-sequencing and transcriptome read alignment**

535 Total RNA was extracted from fresh cells or frozen tumors using TRIzol® Reagent (Invitrogen),

536 or AllPrep DNA/RNA Mini Kit (Qiagen) or NucleoSpin RNA kit (Macherey-Nagel; for the SK-
537 N-SH cell line treated with chemotherapy). All samples were subjected to quality control on a
538 Bioanalyzer instrument and only RNA with RIN (RNA Integrity Number) > 6 were used for
539 sequencing. RNA sequencing libraries were prepared from 1 µg of total RNA using the Illumina
540 TruSeq Stranded mRNA Library preparation kit which allows performing a strand-specific
541 sequencing. A first step of polyA selection using magnetic beads is done to focus sequencing on
542 polyadenylated transcripts. After fragmentation, cDNA synthesis was performed and resulting
543 fragments were used for dA-tailing and then ligated to the TruSeq indexed adapters. PCR
544 amplification is finally achieved to create the final cDNA library. After qPCR quantification,
545 sequencing was carried out using 2 x 50 cycles (paired-end reads 50 nts) for all samples (except
546 SH-EP, 2 x 100; Pair1-Relapse and Pair3-Relapse, 2 x 75; Pair2-Relapse, 2 x 150). Sequencing
547 was performed with the Illumina HiSeq2500 instrument (high output mode) except for cases
548 Pair1-Relapse and Pair2-Relapse analyzed with the NextSeq500 instrument and Pair3-Relapse3
549 analyzed on a HiSeq4000 instrument. Reads were aligned to the human reference genome
550 hg19/GRCh37 using TopHat2 v2.0.6[43] with the following parameters: global alignment, no
551 mismatch in the 22 bp seed, up to three mismatches in the read, library type fr-firststrand.
552 Gene expression values (FPKM=fragments per kilobase per million reads) were computed by
553 Cufflinks v2.2.1[44] and further normalization between samples was done using quantile
554 normalization (R/Bioconductor package limma)[45].
555
556 **Western blots**
557
558 Western blots were carried out using standard protocols with the following antibodies: PHOX2B
559 (sc-376997 from Santa Cruz Biotechnology at 1:500) and anti-vinculin (ab18058 from Abcam at
560 1:1,000). Membranes were then incubated with an anti-mouse immunoglobulin G (IgG)
561 horseradish peroxidase–coupled secondary antibody (1:3,000, NA931V) from GE Healthcare.
562 Proteins were detected by enhanced chemiluminescence (PerkinElmer).
563
564 **Single cell gene expression analysis**

565 Single cells loading, capture and mRNA pre-amplification were performed following the
566 Fluidigm user manual "Using C1 to Capture Cells from Cell Culture and Perform

567 Preamplification Using Delta Gene Assays”. Briefly, cells were dissociated using TrypLE
568 Express reagent (Gibco), washed 2 times in PBS and 2,000-4,000 cells were loaded onto a
569 medium size (10-17µm) C1 single-cell auto prep IFC (Fluidigm). The capture efficiency was
570 assessed by imaging capture sites under the microscope and cell viability was investigated with
571 ethidium homodimer-1 and calcein AM stains (LIVE/DEAD kit, Thermo Fisher Scientific).
572 Capture sites containing more than one cell or a dead cell were later excluded. Lysis, reverse
573 transcription, and specific target preamplification steps were done on the C1 machine according
574 to the Fluidigm user manual. Preamplification was done with inventoried pairs of unlabeled
575 primers coupled with a Taqman probe FAM-MGB (Applied Biosystems TaqMan Gene
576 Expression Assays, Thermo Fischer Scientific) for each of the module 1 and 2 genes and 4
577 housekeeping genes (GAPDH, ACTG1, ACTB and RPL15). Preamplification products were
578 harvested and high throughput real-time PCR was performed using the Fluidigm Biomark HD
579 system with 48.48 gene expression Dynamic Arrays. For each cell line, a bulk control
580 representative of 400 cells was processed the same way as the single cells. The raw data were
581 first analyzed with the Fluidigm Real-Time PCR Analysis Software and exported to csv files for
582 further analysis.
583 Gene expression value was normalized using the geometric mean of all 4 housekeeping genes Ct
584 values of a given cell, cells were excluded if this geometric mean was >16.5. The Livak method
585 ($2^{-\Delta\Delta Ct}$) was applied using the gene expression values of the SK-N-SH cell line population as
586 reference for the relative expression. Hierarchical clustering was performed using one minus
587 Pearson correlation with an average linkage method including heatmap using Morpheus platform
588 (https://software.broadinstitute.org/morpheus).
589
590 **Treatment of cell lines with chemotherapy**

591 SH-EP and SH-SY5Y cell lines were plated in 96-well plates two days before the addition of
592 cisplatin, etoposide or doxorubicin. Seeding densities for each cell lines were optimized to reach
593 80% of confluency in the untreated cells. Cells were treated with chemotherapeutic agents for 48
594 h. Cell viability was then measured using the *in vitro* Toxicology Assay Kit, Resazurin-based,
595 following manufacturer’s instructions (Sigma-Aldrich).

596 SK-N-SH cells were plated in 6-well plates and then treated with cisplatin (7.5 µM) or

597 doxorubicin (100 nM) for 7 days, medium and drugs were changed every 2 days. RNAs were
598 extracted using NucleoSpin RNA kit (Macherey-Nagel).

599 **Doxycycline-inducible shRNA systems**

600 PHOX2B-specific short hairpin RNAs sh1783 (5'-CCGGTGGAAGGCAGAAACCATTAAA-
601 CTCGAGTTTAATGGTTTCTGCCTTCCATTTTTG-3') and sh1437 (5'-CCGGAGTAATCG-
602 CGCTAAGAATAAACTCGAGTTTATTCTTAGCGCGATTACTTTTTG-3') were selected
603 from Sigma Mission shRNA library and cloned into the pLKO-Tet-On all-in-one system[46]
604 (Addgene). Lentiviral particles were produced in HEK293T cells and CLB-GA cells were
605 infected as previously described[4]. SH-SY5Y cells were incubated with viral particules for 48
606 hours without polybrene. Selection with puromycin (Invitrogen) at 400 ng/ml or 1 µg/ml,
607 respectively, was performed 24 h after infection and maintained during all culture experiments,
608 for CLB-GA and SH-SY5Y cells, respectively. PHOX2B knockdown efficacy was assessed by
609 Western blot 24 h/48 h/96 h after the addition of doxycycline (100 ng/ml or 1 µg/ml). For colony
610 formation assays, $6x10^4$ transduced cells were plated at day 0 in 6-well dishes and stained with
611 crystal violet at day 11[47].

612 **Proliferation assays**

613 Cells were counted in real-time with an xCELLigence™ instrument (ACEA Biosciences)
614 monitoring imped-ance across gold microelectrodes. 10^4 infected CLB-GA or SH-SY5Y cells
615 were seeded per well of a 96-well plate in 200 µl medium containing doxycycline at 100 ng/ml
616 or 1 µg/ml (quintuplicates per group) or no doxycycline. Medium was refreshed after 48 h. For
617 cell counting, $2x10^4$ infected CLB-GA or 10^5 infected SH-SY5Y were plated in 24-well plates in
618 the presence or absence of doxycycline at 100 ng/ml or 1 µg/ml. The number of living cells was
619 counted at day 4, 7, 10 and 14 (triplicates per group) for CLB-GA and at day 8 (n=5/6 technical
620 replicates) for SH-SY5Y cells using a Vi-cell XR Cell Viability Analyzer (Beckman Coulter)
621
622

623 **Statistical analysis**

624 To calculate p-values for Pearson correlation (null hypothesis consisted in zero Pearson
625 correlation), we implemented a one-sided permutation test. Number of permutations was 10^4

626 when calculating p-values for correlation between SE score and gene expression (Figure S11)
627 and 10^6 in the test for correlation between gene expression of the noradrenergic and NCC-like
628 modules in the set of tumors (Figure 2). This test does not need the data to follow the normal
629 distribution and does not require equal variation between the groups that are statistically
630 compared.
631

632 **Xenotransplantation experiments and mice**

633 10 x 10^6 CLB-GA cells transduced with the shRNA against PHOX2B (sh1783) were injected
634 subcutaneously in the flanks of 6-week-old NSG mice (Charles Rivers Laboratories) in an equal
635 mix of PBS and Matrigel (BD Biosciences). When tumors reached a volume of around 170 mm^3,
636 mice were randomly assigned to the control (5% sucrose in drinking water) or the treatment
637 (doxycycline (2 mg/l) and 5% sucrose in drinking water) groups. Tumor growth was monitored
638 with a caliper every day. Mice were killed once tumors reached a volume of around 3,000 mm^3
639 calculated as $V = a/2 \times b \times ((a+b)/2)$ with a being the largest diameter and b the smallest.
640 Experiments were conducted in accordance with the recommendations of the European
641 Community (86/609/EEC), the French Competent Authority, and UKCCCR (guidelines for the
642 welfare and use of animals in cancer research). Approval for this study was received from
643 Ministère de l’Education Nationale, de l'Enseignement Supérieur et de la Recherche
644 (authorization number 5524-20 160531 1607151 v5).
645

646 **PHOX2B immunohistochemistry**

647 Mice tumors were fixed with acidified formal alcohol (AFA) for 24 h and paraffin-embedded.
648 Labelling was performed on 4 µm sections with the BOND-III instrument (Leica Microsystems)
649 using the Bond Polymer Refine Detection™ (Leica) kit. Briefly, sections were deparaffinized,
650 antigen retrieval was performed with an EDTA-based solution (Leica) for 20 minutes at pH 9,
651 and sections were stained with a rabbit polyclonal anti-PHOX2B antibody (Abcam, EPR14423,
652 1/1000).
653

654 **siRNA and growth assays**

655 HAND2 and GATA3 knockdown was performed with 20 nM siRNA (Hs_HAND2_3
656 #SI00131915, Hs_HAND2_6 #SI03046736, Hs_GATA3_7 #SI04202681 and Hs_GATA3_8

#SI04212446; Control siRNA #1027281; Qiagen) using RNAimax transfection reagent (Thermo Fisher Scientific). The number of living cells was counted using a Vi-cell XR Cell Viability Analyzer (Beckman Coulter) (n=5 or 6 technical replicates).

Data Availability

Raw data for cell line ChIP-seq and RNA-seq, and processed data for the cell lines, tumors and PDXs are available in Gene Expression Omnibus (GEO) under accession number GSE90683. Raw data for PDX ChIP-seq and RNA-seq will be available through EGA, as well as RNA-seq data for patient samples.

Reviewers can access to the GEO submission using this link: https://www.ncbi.nlm.nih.gov/geo/query/acc.cgi?token=khcvkaailpulxqt&acc=GSE90683.

Code availability

The code of the pipeline for the SE detection from cancer ChIP-seq data is available at http://boevalab.com/LILY/ .

30. Schleiermacher, G. *et al*. Combined 24-color karyotyping and comparative genomic hybridization analysis indicates predominant rearrangements of early replicating chromosome regions in neuroblastoma. *Cancer Genet Cytogenet* **141**, 32-42 (2003)

31. Boeva, V. *et al.* Control-free calling of copy number alterations in deep-sequencing data using GC-content normalization. *Bioinformatics* **27,** 268–9 (2011).

32. Etchevers, H. Primary culture of chick, mouse or human neural crest cells. *Nat. Protoc.* **6,** 1568–1577 (2011).

33. Monterrubio, C. *et al.* Targeted drug distribution in tumor extracellular fluid of GD2-expressing neuroblastoma patient-derived xenografts using SN-38-loaded nanoparticles conjugated to the monoclonal antibody 3F8. *J. Control. Release* **255,** 108–119 (2017).

34. Vassal, G. *et al.* Therapeutic activity of CPT-11, a DNA-topoisomerase I inhibitor, against peripheral primitive neuroectodermal tumour and neuroblastoma xenografts. *Br. J. Cancer* **74,** 537–545 (1996).

35. Bettan-Renaud, L., Bayle, C., Teyssier, J. R. & Benard, J. Stability of phenotypic and

687 genotypic traits during the establishment of a human neuroblastoma cell line, IGR-N-835. *Int. J.*
688 *Cancer* **44,** 460–466 (1989).
689 36. Langmead, B. & Salzberg, S. L. Fast gapped-read alignment with Bowtie 2. *Nat. Methods* **9,**
690 357–359 (2012).
691 37. Ashoor, H. *et al.* HMCan: a method for detecting chromatin modifications in cancer samples
692 using ChIP-seq data. *Bioinformatics* **29,** 2979–2986 (2013).
693 38. ENCODE Project Consortium. An integrated encyclopedia of DNA elements in the human
694 genome. *Nature* **489,** 57–74 (2012).
695 39. Lovén, J. *et al.* Selective inhibition of tumor oncogenes by disruption of super-enhancers.
696 *Cell* **153,** 320–334 (2013).
697 40. Rao, S. S. P. *et al.* A 3D map of the human genome at kilobase resolution reveals principles
698 of chromatin looping. *Cell* **159,** 1665–1680 (2014).
699 41. Herrmann, C., Van de Sande, B., Potier, D. & Aerts, S. i-cisTarget: an integrative genomics
700 method for the prediction of regulatory features and cis-regulatory modules. *Nucleic Acids Res.*
701 **40,** e114 (2012).
702 42. Medina-Rivera, A. *et al.* RSAT 2015: Regulatory Sequence Analysis Tools. *Nucleic Acids*
703 *Res.* **43,** W50-56 (2015).
704 43. Kim, D. *et al.* TopHat2: accurate alignment of transcriptomes in the presence of insertions,
705 deletions and gene fusions. *Genome Biol.* **14,** R36 (2013).
706 44. Trapnell, C. *et al.* Transcript assembly and quantification by RNA-Seq reveals unannotated
707 transcripts and isoform switching during cell differentiation. *Nat. Biotechnol.* **28,** 511–515
708 (2010).
709 45. Ritchie, M. E. *et al.* limma powers differential expression analyses for RNA-sequencing and
710 microarray studies. *Nucleic Acids Res.* **43,** e47 (2015).
711 46. Wiederschain, D. *et al.* Single-vector inducible lentiviral RNAi system for oncology target
712 validation. *Cell Cycle* **8,** 498–504 (2009).
713 47. Franken NAP, Rodermond HM, Stap J, Haveman J, van Bree C. Clonogenic assay of cells in
714 vitro. Nat Protoc. 2006; 1:2315–2319.
715
716
717

Acknowledgements

This work was supported by grants from Institut Curie, Inserm, the Ligue Nationale Contre le Cancer (Equipe labellisée), the Société Française de Lutte contre les Cancers et les Leucémies de l'Enfant et l'Adolescent, the Institut National du Cancer (PRT-K14-061), the PHRC IC 2007-2009) and by the following associations: Association Hubert Gouin, Les Bagouz à Manon, les amis de Claire, Courir pour Mathieu, Dans les pas du Géant, Olivier Chape. The Mappyacts protocol is supported by the PRHC, the Fondation ARC, the Société Française de Lutte contre les Cancers et les Leucémies de l'Enfant et l'Adolescent (Fondation Enfants & Santé), the Fondation AREMIG and the Association Thibault BRIET). High-throughput sequencing has been performed by the ICGex NGS platform of the Institut Curie supported by the grants ANR-10-EQPX-03 (Equipex) and ANR-10-INBS-09-08 (France Génomique Consortium) from the Agence Nationale de la Recherche ("Investissements d'Avenir" program), by the Canceropole Ile-de-France and by the SiRIC-Curie program -SiRIC Grant "INCa-DGOS- 4654". Biomark analysis was done using the High Throughput qPCR-HD-Genomic Paris Centre platform supported by grants from "Région Ile-de-France". G.S. is supported by the Annenberg foundation. V.B. is supported by the ATIP-Avenir Program, the ARC Foundation (grant ARC - RAC16002KSA - R15093KS), Worldwide Cancer Research Foundation (grant WCR16-1294 R16100KK) and the "Who Am I?" laboratory of excellence ANR-11-LABX-0071 funded by the French Government through its "Investissement d'Avenir" program operated by The French National Research Agency (ANR) (grant ANR-11-IDEX-0005-02). H.R. is supported by the Mayent-Rothschild program from Institut Curie and the Wilhelm-Sander-Stiftung. The laboratory of T.G.P.G. is supported by LMU Munich's Institutional Strategy LMUexcellent within the framework of the German Excellence Initiative, the 'Mehr LEBEN für krebskranke Kinder – Bettina-Bräu-Stiftung', the Walter Schulz Foundation, the Wilhelm-Sander-Stiftung (2016.167.1), and by the German Cancer Aid (DKH-111886 and DKH-70112257). We are grateful to M. Ponzoni (Genova, Italy) for providing the GICAN cell line, F. Tirode and C. Kamoun for help with RNA-seq analysis and alignment of NGS data, respectively, O. Blanchard for help in cell culture experiments and M. Caly for PHOX2B immunohistochemistry. We are grateful to the animal facilities team, the Experimental Pathology Department and the Plateforme

749 Génomique of Institut Curie. We thank N. Clément, T. Adam-de-Beaumais and B. Mallon for
750 their help in the identification of neuroblastoma diagnosis/relapse pairs and V. Bernard for pairs
751 validation. We thank V. Saint-André for scientific discussion, J. Maliash-Planchon and the Unité
752 de Génétique Somatique for preparation of patient samples. We thank Pr. Figarella-Branger (BB-
753 033-00097, CRB AP-HM, CRB TBM, AC-2013-1786), M. Clapisson (CRB Centre Léon Bérard,
754 AC-2008-101), Dr Minckes, Dr Blanc-Fournier and N. Rousseau (CHU, Tumorothèque - Caen
755 Basse-Normandie) for providing tumor patient samples.
756

757 **Author information**

758 **Contributions**

759 V.B. and I.J-L. conceived the study, analyzed the data and wrote the manuscript. V.B.
760 coordinated bioinformatics analysis and I.J.-L. coordinated the whole study. C.L. performed *in*
761 *vitro* experiments and all ChIP experiments and participated in the study design. A.P. generated
762 and analyzed the doxycycline-inducible anti-*PHOX2B* shRNA cell lines. S.D. performed the
763 single cell analysis and study of chemotherapeutic agents. C.P.-E. performed the *in vivo*
764 experiments and contributed *in vitro* experiments.V.R. performed all sequencing experiments.
765 H.E. and S.T. provided hNCC cell lines and V.C. provided neuroblastoma cell lines. A.L.
766 performed alignment of RNA-seq and ChIP-seq data. E.D.-D., B.G., D.S. and A.M.C. provided
767 neuroblastoma PDXs. I.M. performed the reproducibility analysis. E.D. and B.D. generated the
768 Biomark data. M.F.O. and T.G.P.G. generated lentiviral particles and provided help with
769 lentiviral infections. S.B. coordinated and supervised sequencing experiments. G.S. participated
770 in the study design and provided the in-house pairs of diagnosis/relapse samples with the help of
771 E.L., G.P. and B.G. S.G.-L. participated in RNA-seq analysis. E.B. provided computational
772 infrastructure and data storage. H.R. and T.D. provided expertise in sympathetic nervous
773 development and transcription factors. I.J.-L and O.D. provided laboratory infrastructure. I.J.-L,
774 V.B. and O.D. provided financial support. All authors read and approved the final manuscript.

775

776 **Competing financial interests**

777 The authors declare no competing financial interests.

778

779 **Corresponding authors**

780 Correspondence to:

781

782 - Valentina Boeva: valentina.boeva@inserm.fr
783 - Isabelle Janoueix-Lerosey: janoueix@curie.fr

784

785

786

787

788

789

790

791

792 **Extended data figures and tables**

793

794 **Supplementary Table 1**: *MYCN, ALK* and *PHOX2B* status of neuroblastoma cell lines and
795 PDXs. Amp., amplification; Non amp., non amplified; WT, wild-type. NA: not available.
796 * As determined by Sanger sequencing of exons 23 and 25.
797 ¤ MYCN locus: 5 copies; MYC locus: 7 copies; ALK locus: 7 copies (from Control-FREEC
798 analysis)
799 # In frame deletion in the second PolyAlanine track; functional change unknown.

800

801 **Supplementary Table 2:** Patient clinical data.

802

803 **Supplementary Table 3**: Characteristics of neuroblastoma and hNCC super-enhancers. Group I:
804 all neuroblastoma cell lines with the exception of SH-EP, GIMEN, GICAN, SK-N-AS, SJNB12,
805 SK-N-SH and CHP-212; Group II: SH-EP, GIMEN and GICAN.

806

807 **Supplementary Table 4**: Supervised analysis of SE scores according to *MYCN* status.

808

809 **Supplementary Table 5**: Supervised analysis of SE scores according to ALK status.

810

811 **Supplementary Table 6**: Raw Ct values measured for housekeeping genes (GAPDH, ACTG1,
812 ACTB, RPL15) and TFs of modules 1 and 2 for single cells of the SK-N-AS, SH-EP, SH-SY5Y
813 and SK-N-SH cell lines using the Fluidigm Biomark HD.

814

815

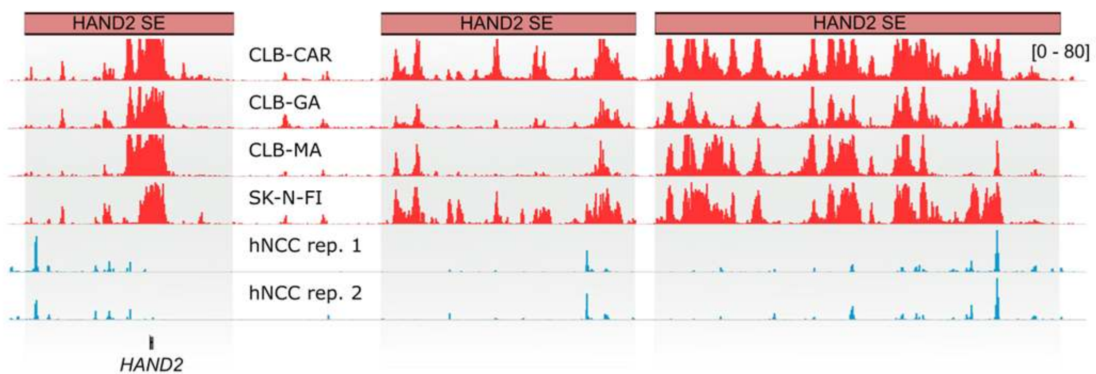

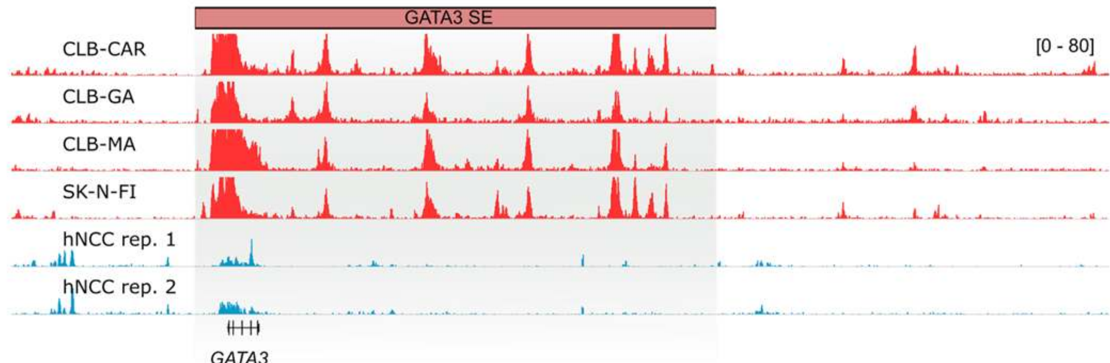

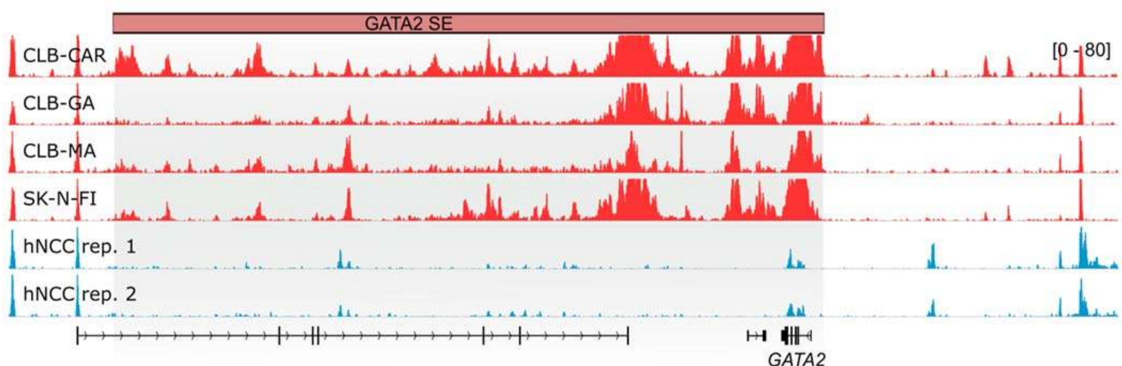

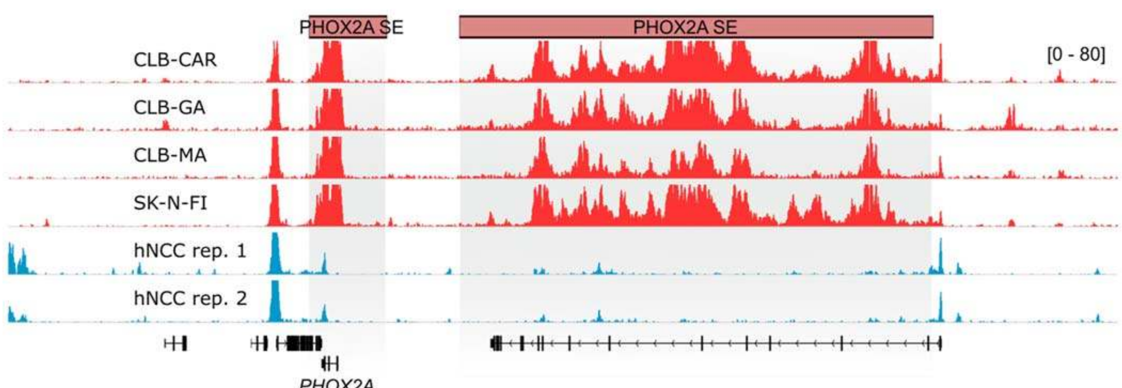

816

817 **Supplementary Figure 1**: Tracks for ChIP-seq profiles of H3K27ac at *HAND2*, *GATA3*,
818 *GATA2*, and *PHOX2A* SEs.
819
820
821
822
823
824
825
826
827
828
829
830
831
832
833

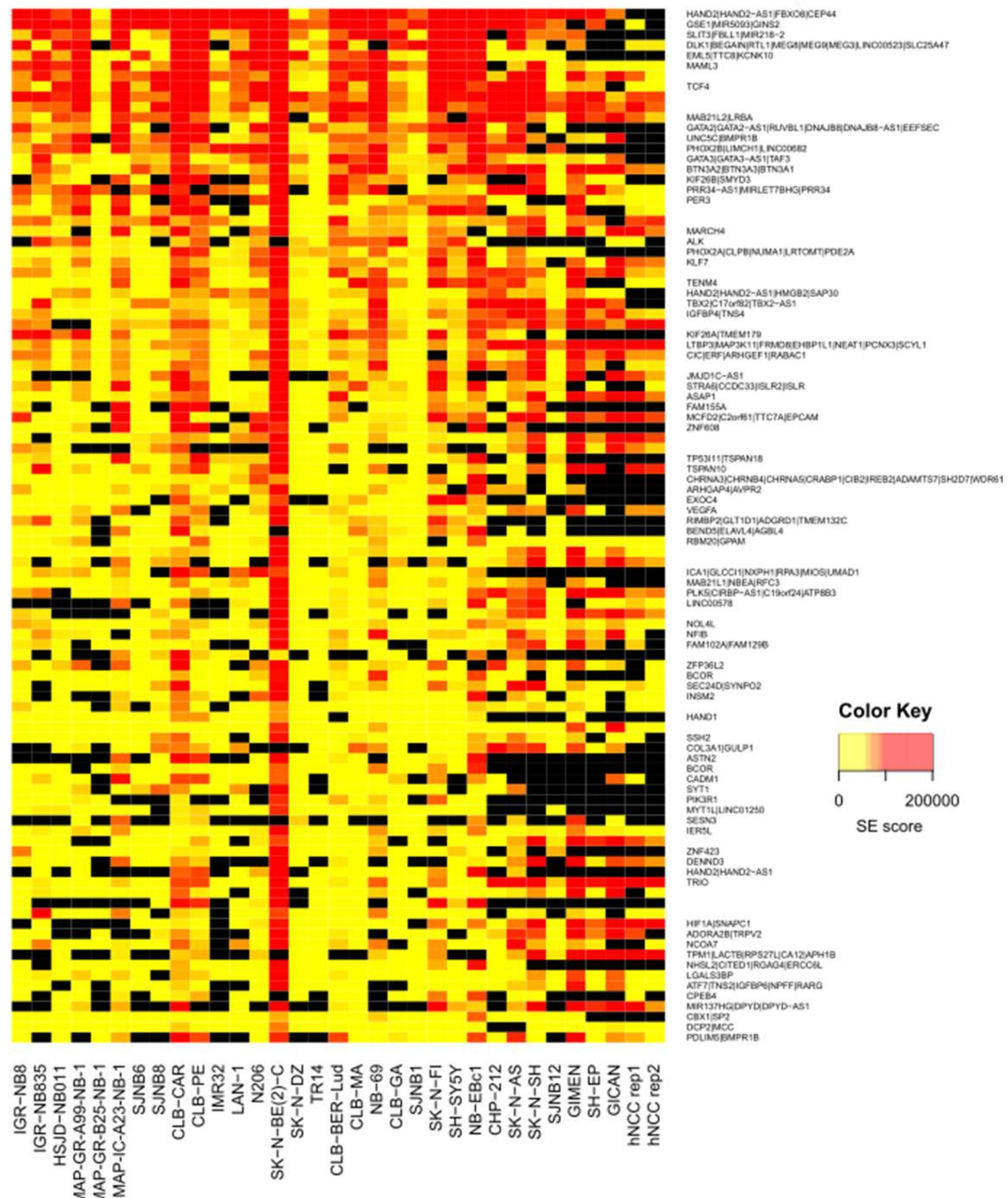

834

835

836 **Supplementary Figure 2:** Heatmap of the SE scores for the 6 PDX, 25 NB cell lines and hNCC

837 cells: top SEs of group I (**a**); top SEs of group II (**b**); SE is not detected (black).

838

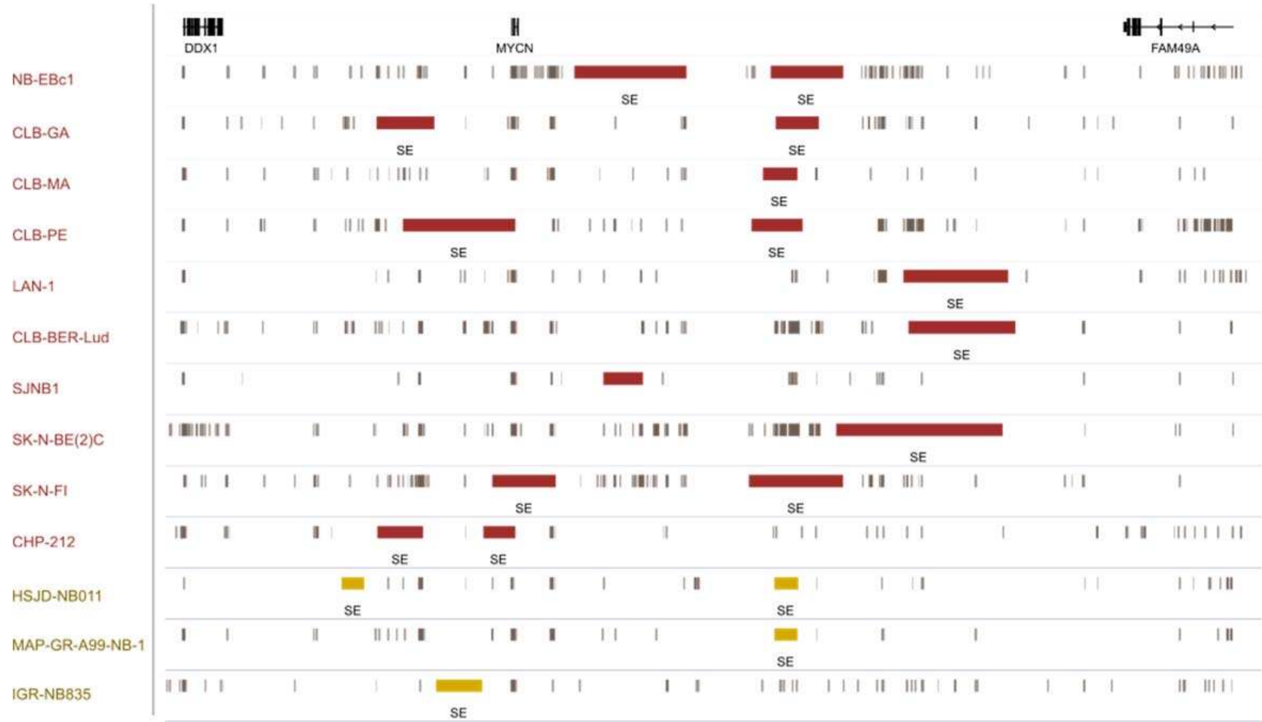

839
840
841

842 **Supplementary Figure 3:** Locations of SE regions predicted for the *MYCN* locus; SEs in NB
843 cell lines (red); SEs in PDX (yellow); typical enhancers and active promoters (grey).

844

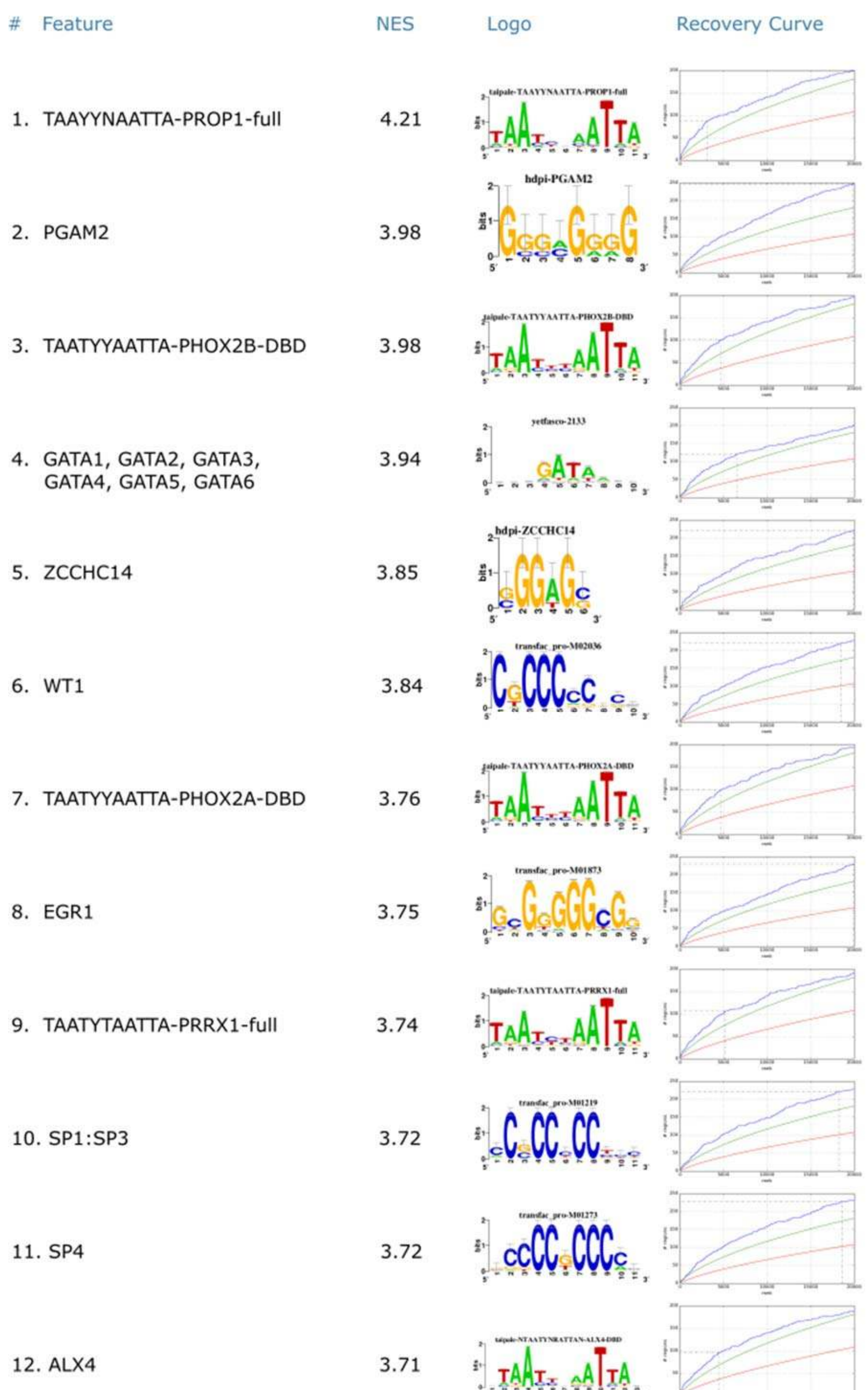

845

846 **Supplementary Figure 4**: i-cis Target summary (database v3.0) on H3K27ac peak valleys of the
847 top 100 strongest SEs identified in group I. NES, Normalized enrichment score. NES threshold
848 3.7. NES and recovery curves are explained at the i-cisTarget website:

849 https://gbiomed.kuleuven.be/apps/lcb/i-cisTarget/ .

850

851

852

853

854

855

856

857

858

859

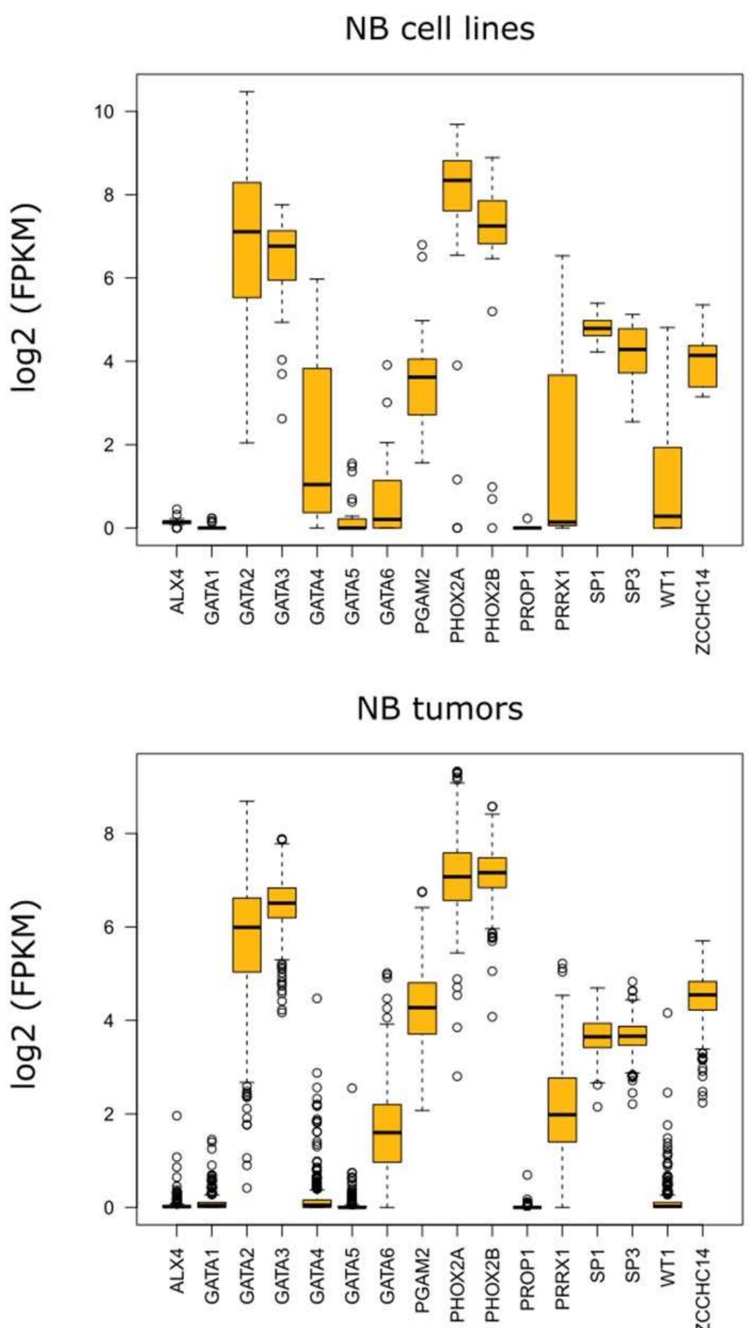

860

861 **Supplementary Figure 5**: Log2 FPKM expression values for genes coding for TFs whose
862 binding motifs are enriched in valleys of H3K27ac peaks of the top 100 strongest SEs identified
863 in group I, in neuroblastoma (NB) cell lines (our data) and NB primary tumors (498 tumors,
864 dataset GSE49711). The box represents the middle 50% of values; the black line inside the box
865 indicates the median.

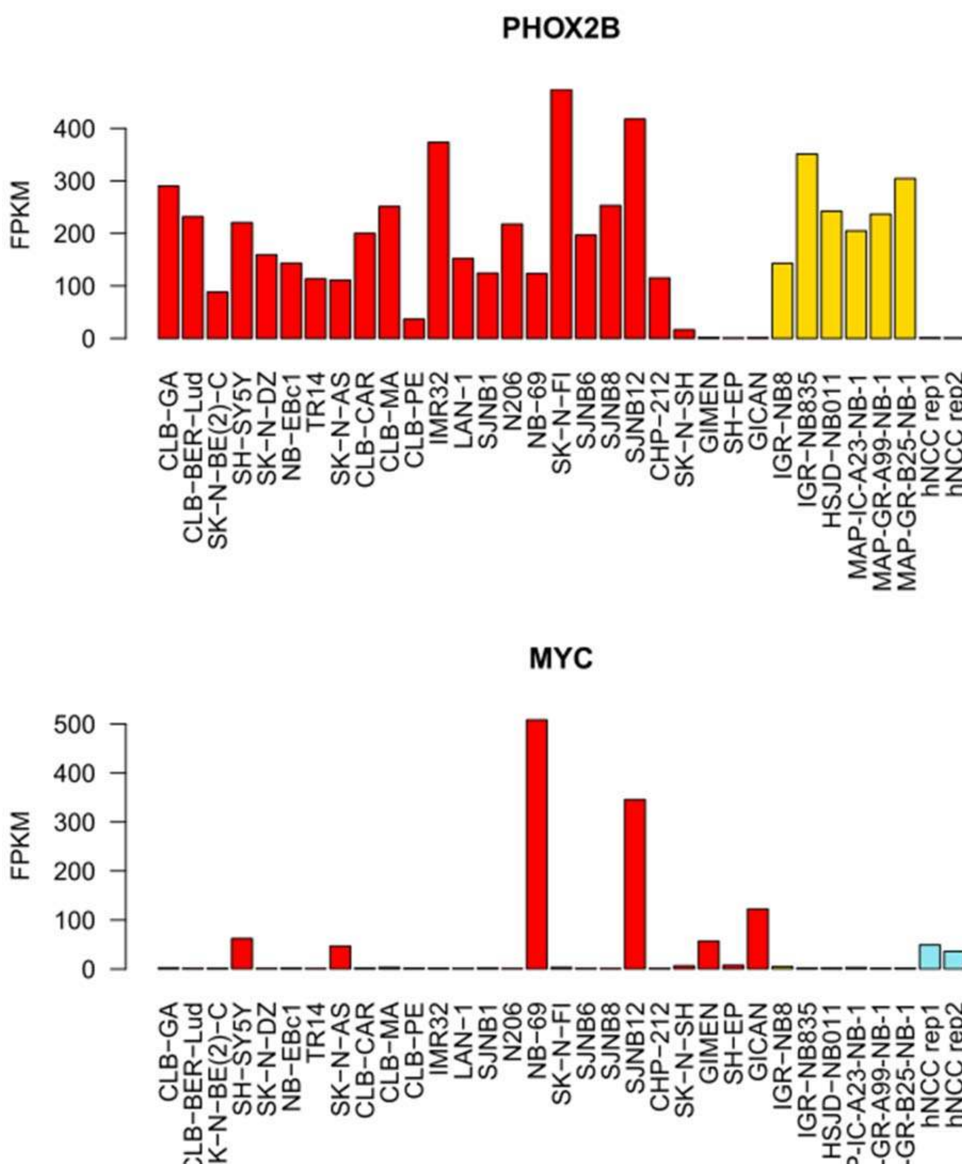

866

867 **Supplementary Figure 6:** *PHOX2B* and *MYC* expression levels measured by RNA-seq in
868 neuroblastoma cell lines (red), PDX (yellow) and hNCC lines (blue).

869

870

871
872

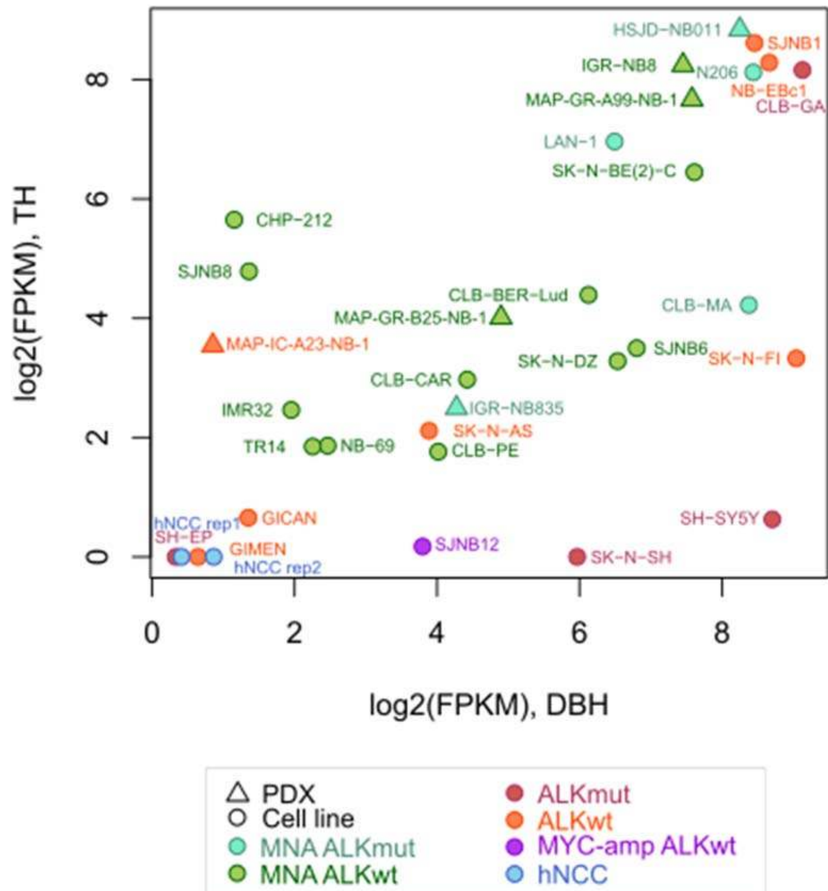

873
874

875 **Supplementary Figure 7:** Log2 FPKM expression values of *DBH* and *TH* in hNCC and
876 neuroblastoma cell lines and PDX measured by RNA-seq.

877
878
879
880
881
882
883

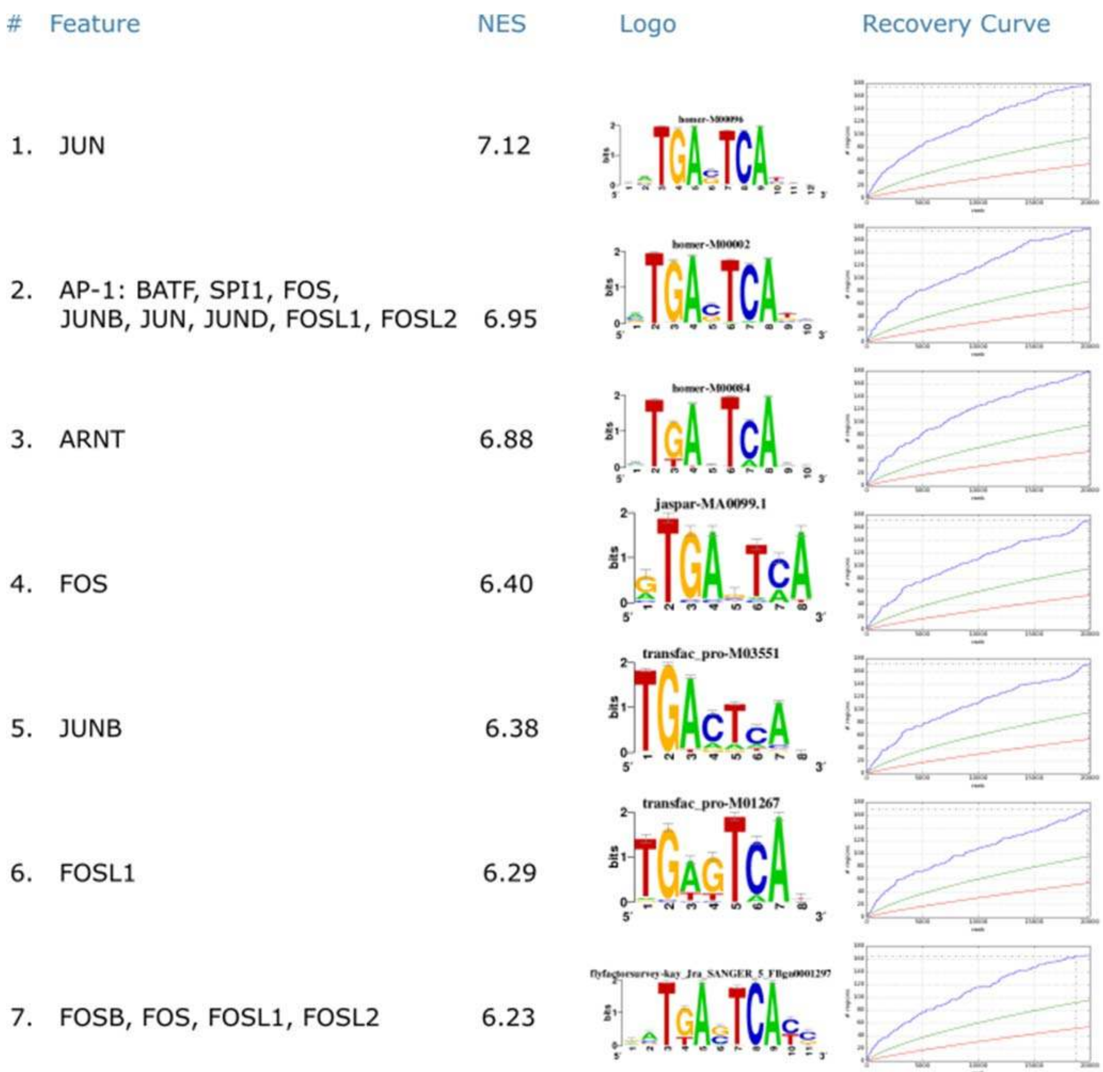

884
885
886
887 **Supplementary Figure 8**: i-cis Target summary (database v3.0) on H3K27ac peak valleys of the
888 top 100 strongest SEs identified in group II. NES, Normalized enrichment score. NES threshold
889 6.2. NES and recovery curves are explained at the i-cisTarget website:
890 https://gbiomed.kuleuven.be/apps/lcb/i-cisTarget/ .

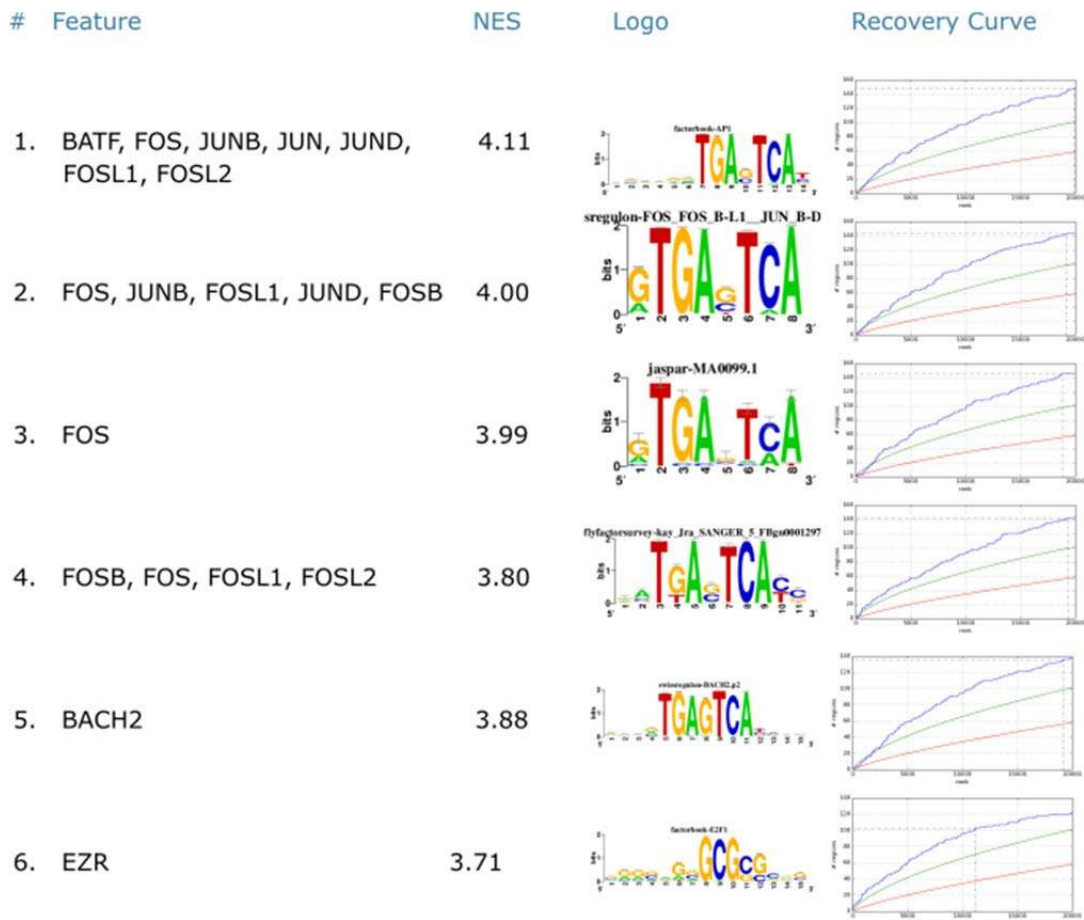

Supplementary Figure 9: i-cis Target summary (database v3.0) on H3K27ac peak valleys of the top 100 strongest SEs identified in hNCC. NES, Normalized enrichment score. NES threshold 3.7. AUC threshold 0.015. NES and recovery curves are explained at the i-cisTarget website: https://gbiomed.kuleuven.be/apps/lcb/i-cisTarget/ .

899

900

901

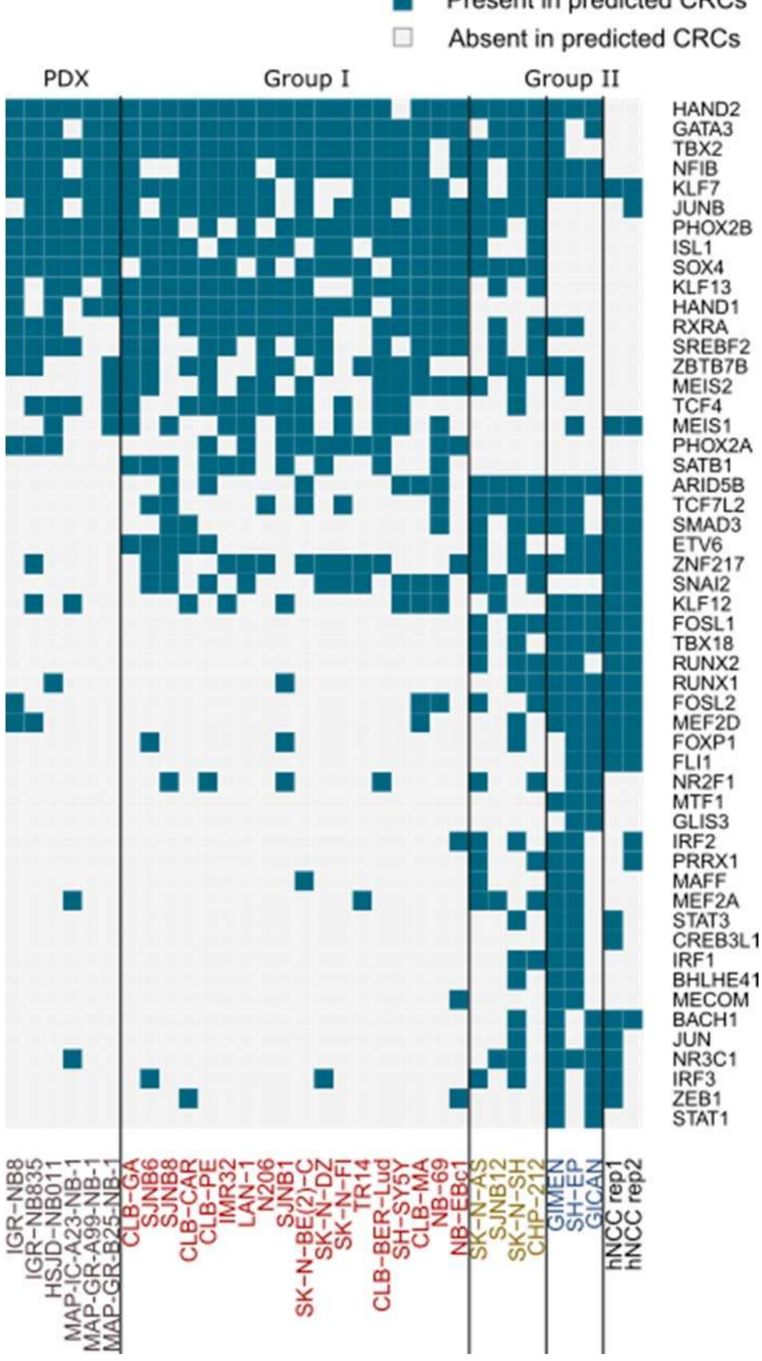

902

903

904 **Supplementary Figure 10**: TFs predicted to participate in CRCs in the two groups of

905 neuroblastoma cell lines, and the primary hNCC.

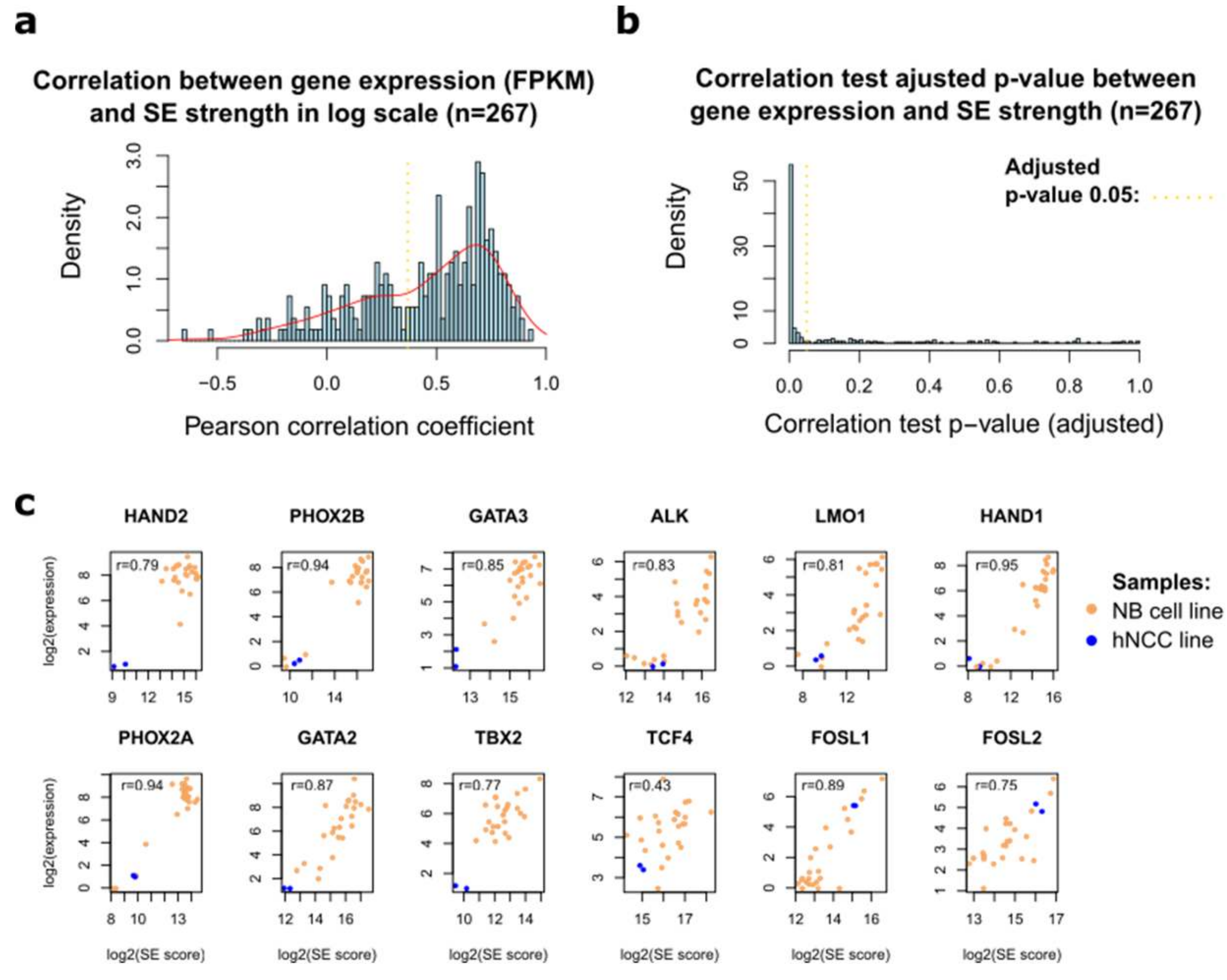

Supplementary Figure 11: Gene expression linearly correlates with SE score (in log scale). **a**, Pearson correlation coefficients were calculated for 267 SE regions corresponding to only one gene and detected in at least 2 neuroblastoma samples. Pearson correlation one-sided permutation tests were performed on the set of 25 neuroblastoma cell lines and 2 hNCC samples; p-values adjusted with the FDR method. **b**, Distribution of corresponding adjusted p-values for 267 SE regions. **c**, Examples of correlation between SE score and expression of particular genes. Orange: neuroblastoma cell lines; blue: hNCC samples.

919

920

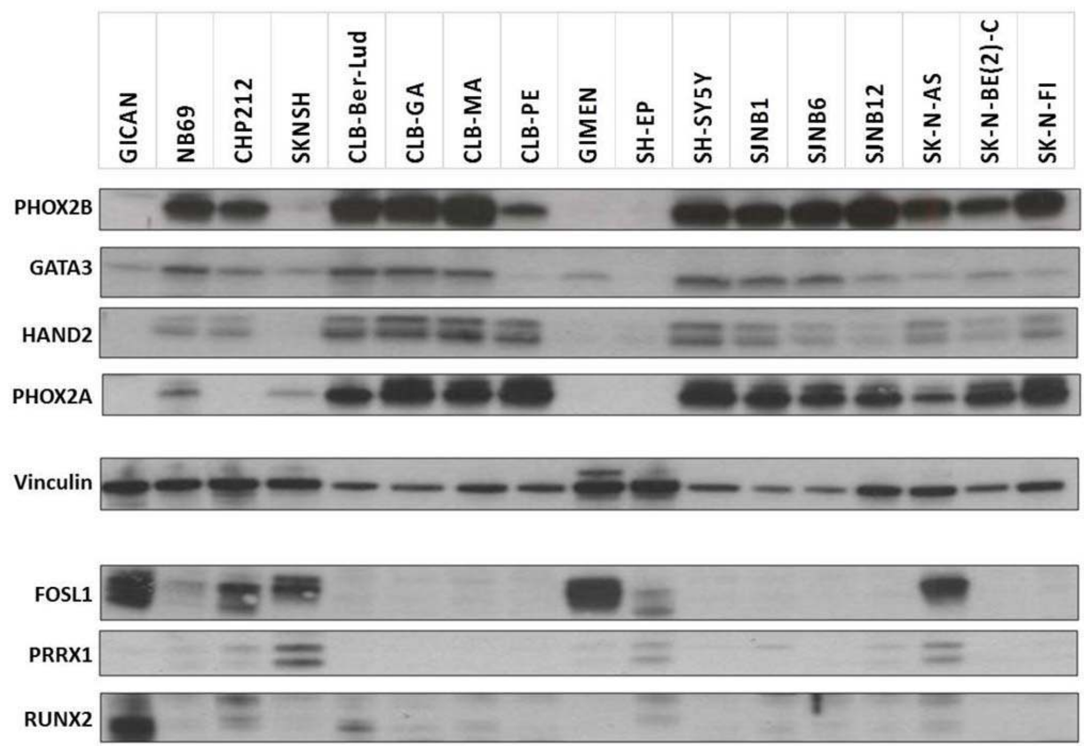

921

922

923

924

925 **Supplementary Figure 12:** Western blot analysis of PHOX2B, GATA3 (CST #5852, D13C9),
926 HAND2 (sc-9409), PHOX2A (sc-8978), FOSL1 (sc-28310), PRRX1 (Sigma HPA051084),
927 RUNX2 (sc-101145) and vinculin in a panel of neuroblastoma cell lines. All antibodies were
928 used at 1:500 except the GATA3 antibody used at 1:1000.

929

930

931

932

933

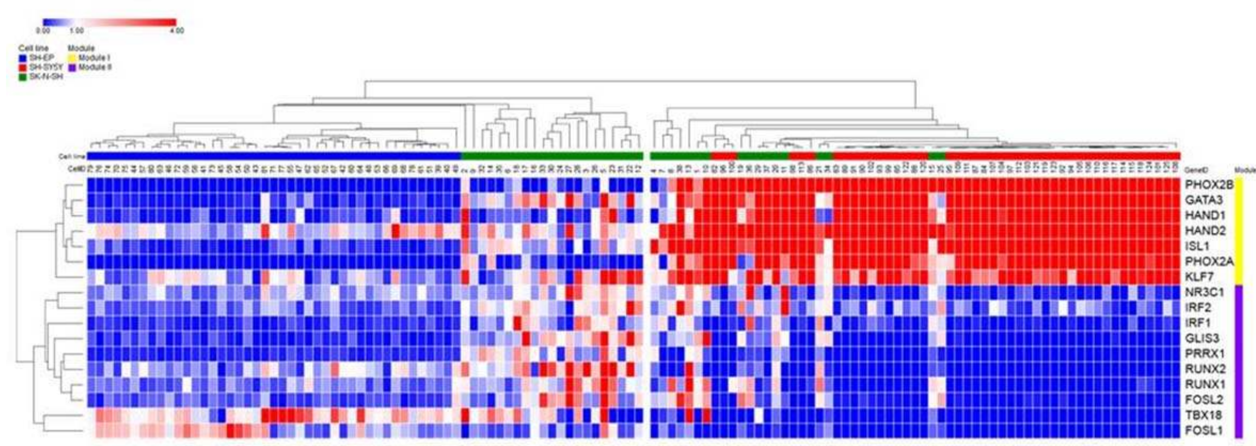

934

935 **Supplementary Figure 13**: Clustering of SK-N-SH, SH-EP and SH-SY-5Y single cells
936 analyzed by RT-q-PCR for the expression of TFs of modules 1 and 2. The first group of cells
937 includes all SH-EP cells as well as some cells of the SK-N-SH cell line; a second group includes
938 all SH-SY5Y cells as well as cells of the SK-N-SH cell line. RT-q-PCR data were normalized to
939 the SK-N-SH cell line population for the three cell lines using the geometric mean of the four
940 housekeeping genes.

941

942

943

944

945

946

947

948

949

950

951

952

953

954

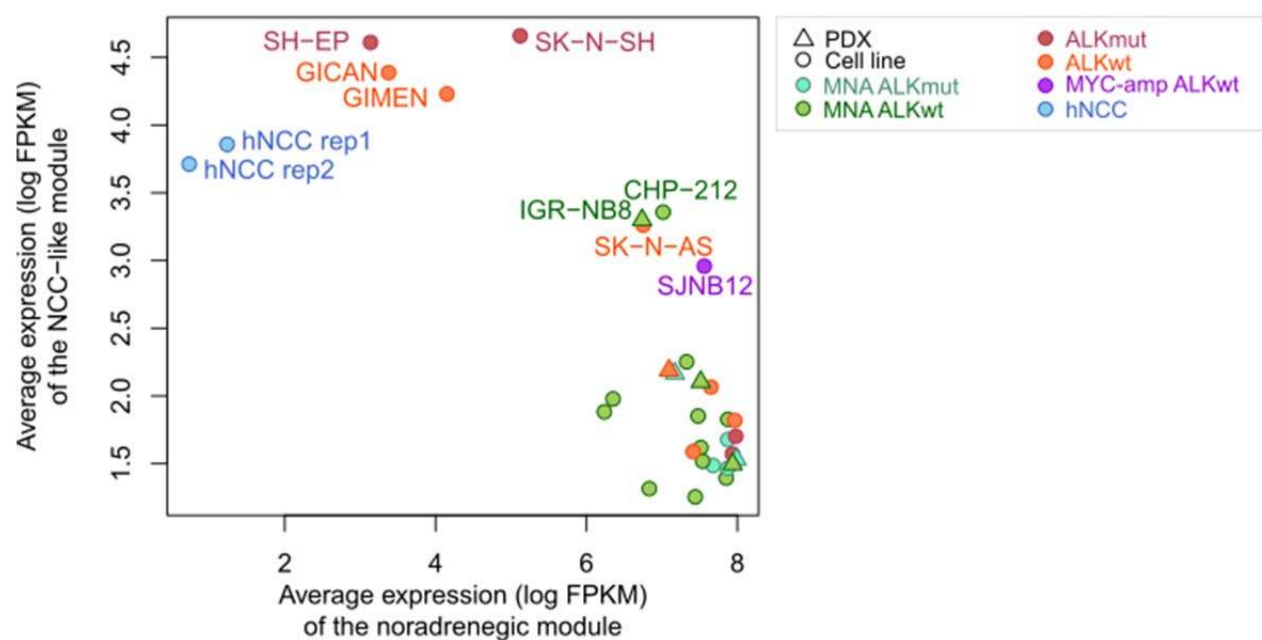

955

956 **Supplementary Figure 14:** Expression of modules 1 and 2 in neuroblastoma cell lines and
957 PDXs. Average is calculated for log2 FPKM values.

958

959

960

961

962

963

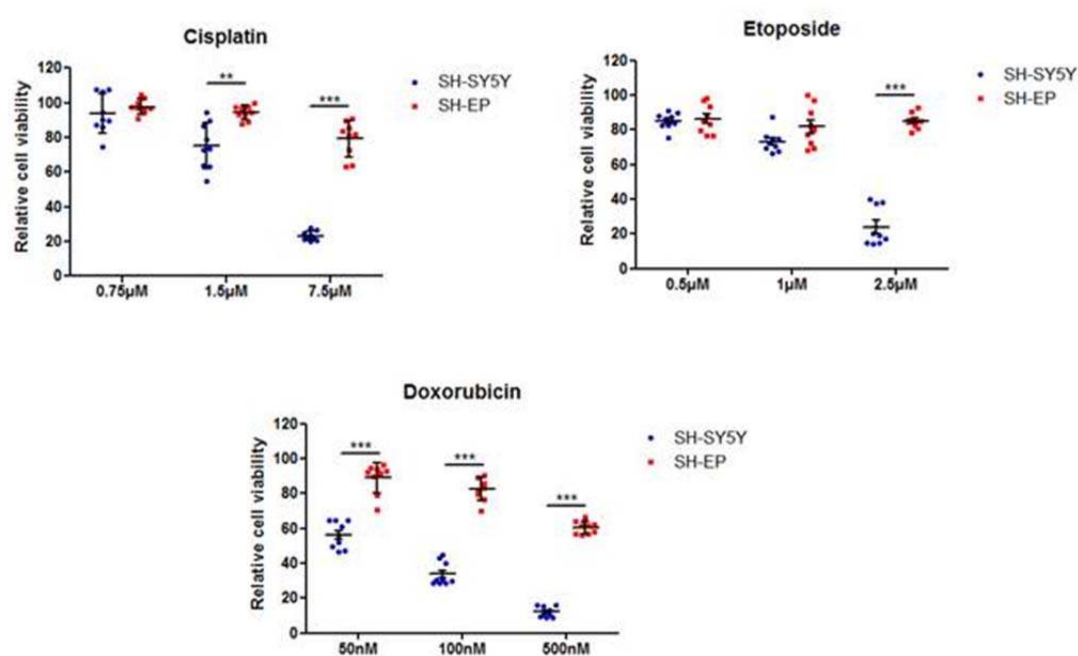

964
965
966 **Supplementary Figure 15:** NCC-like SH-EP cells are more resistant to chemotherapy than
967 noradrenergic SH-SY5Y cells (n=9 technical replicates per condition; P values were determined
968 via two-tailed unpaired Welch's t-test (***: p<0.001)).
969
970
971
972
973

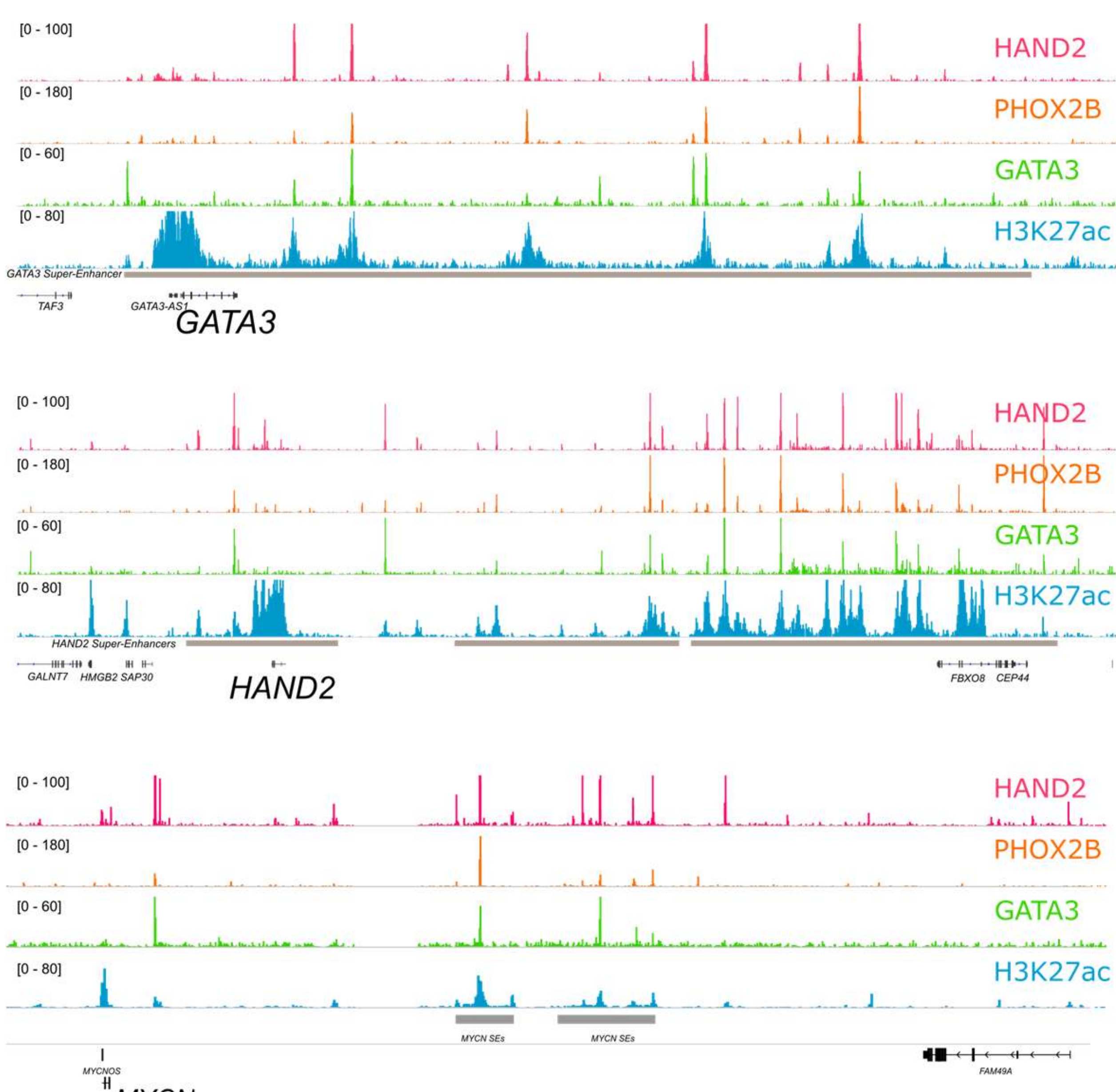

974

975

976

977

978 **Supplementary Figure 16:** Tracks for ChIP-seq profiles for PHOX2B, HAND2, GATA3 and
979 H3K27ac binding at the *GATA3* (top), *HAND2* (middle) and *MYCN* (bottom) SEs in the CLB-
980 GA cell line.

981

982

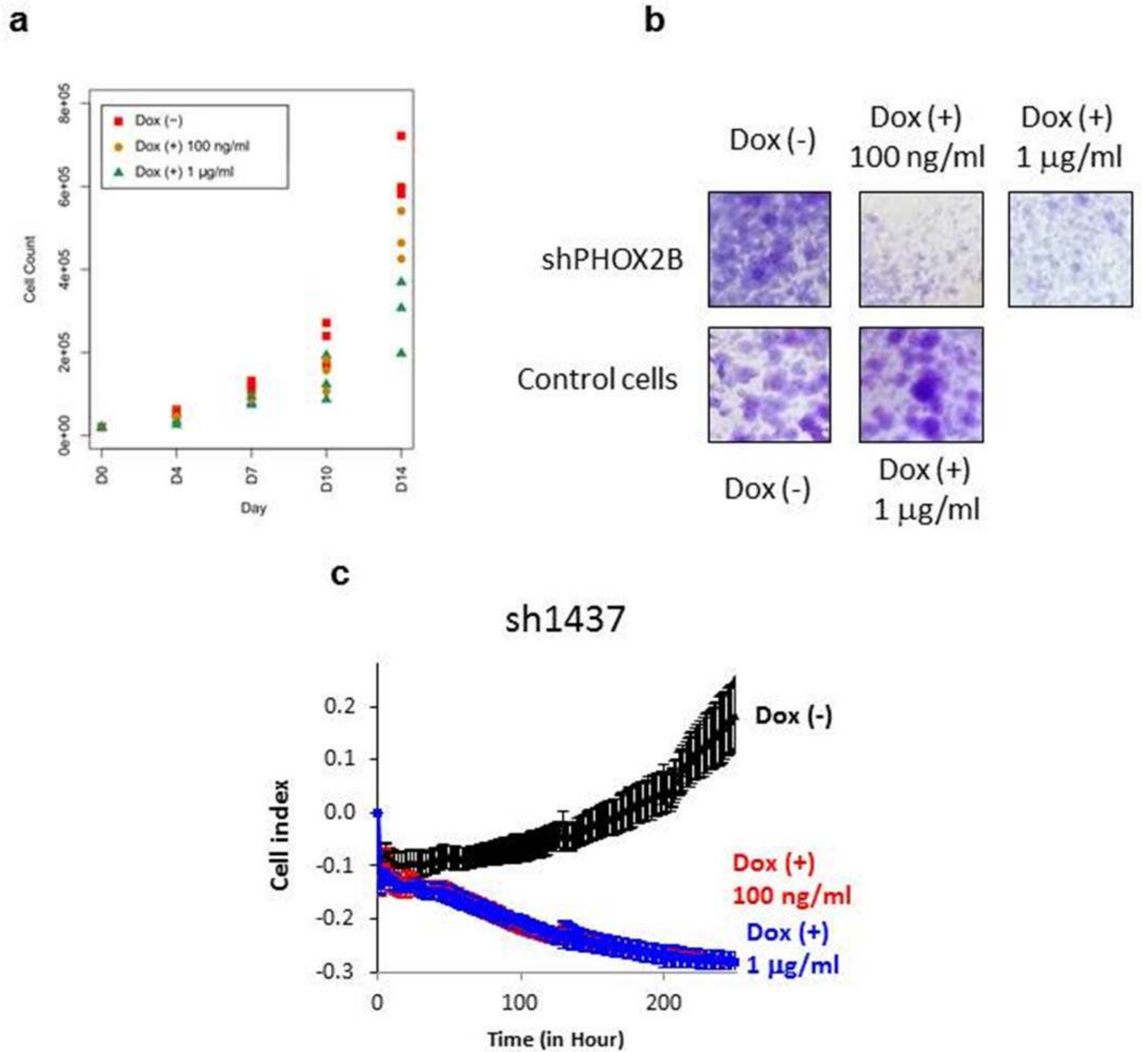

Supplementary Figure 17: a, Validation of xCELLigence™ results by cell counting for the CLB-GA cell line infected with the sh1783 vector targeting PHOX2B. $2x10^4$ cells were plated in 24-well plates at day 0 in the absence or presence of doxycycline at 100 ng/ml or 1 µg/ml. The number of living cells was counted at day 4, 7, 10 and 14. **b,** Decreased foci formation of CLB-GA cells upon doxycycline-induced *PHOX2B* knockdown. Doxycycline at 1 µg/ml did not affect growth of CLB-GA non-infected control cells. **c,** xCELLigence™ proliferation kinetics for the SH-SY5Y cell line infected with the sh1437 vector targeting PHOX2B, respectively. Data shown are the mean ± s.d. of results obtained in the different conditions (n=5 technical replicates)

a

***

5000
4000
3000
2000
1000
0
tumor volum [mm³]
Dox(-)
Dox(+)

b

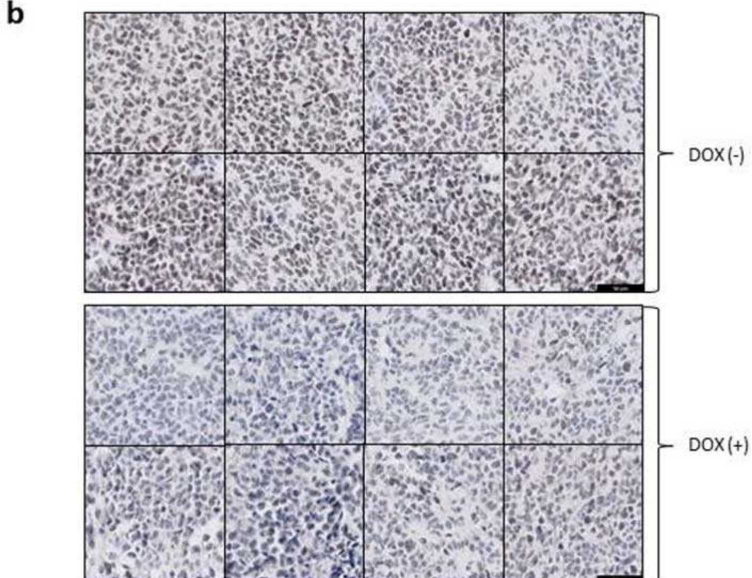

Supplementary Figure 18: a, Tumor volume of mouse xenografts of CLB-GA cells transduced with sh1783 targeting PHOX2B after 11 days of treatment with sucrose alone (Dox(-)) or doxycycline and sucrose (Dox(+)). **b,** PHOX2B expression analyzed by immunohistochemistry (EPR14423-Abcam) in mouse xenografts of CLB-GA cells transduced with sh1783 targeting PHOX2B treated or not with doxycycline (DOX). Each panel corresponds to a different tumor (n=8 tumors in each group).

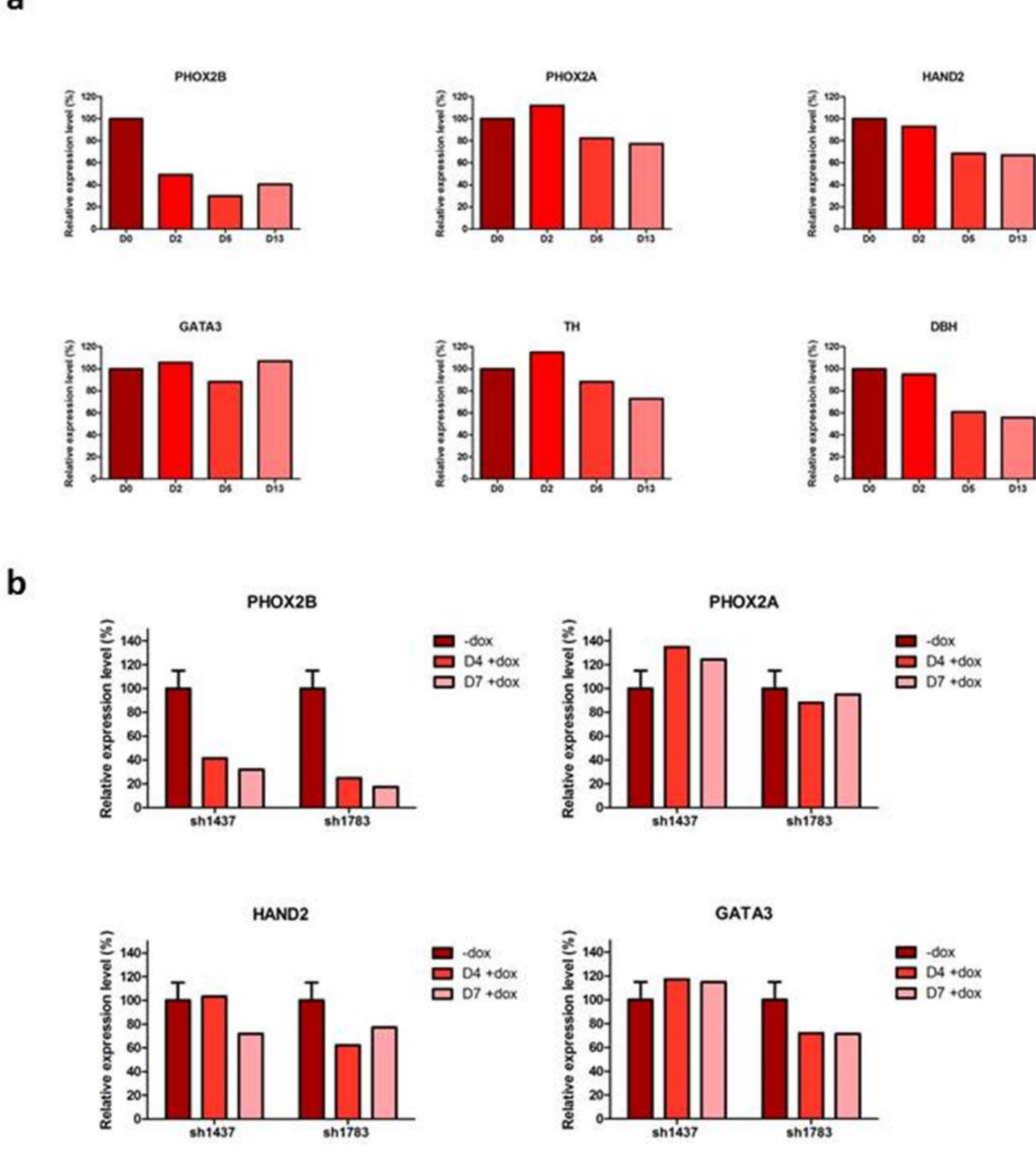

Supplementary Figure 19: Impact of PHOX2B decrease on the expression profiles of CLB-GA and SH-SY5Y cells. **a,** RNA-seq was performed on CLB-GA cells transduced with sh1783 targeting PHOX2B after 2, 5 and 13 days of doxycycline treatment and on untreated cells (D0). Expression levels (FPKM values) for each day are compared to the untreated cells (100%). PHOX2B knockdown resulted in a modest decrease of PHOX2A, HAND2, TH and DBH. No expression of the genes of the NCC-like module was detected in any of the conditions. **b**, Expression of genes of modules 1 and 2 was evaluated by RT-q-PCR on SH-SY5Y cells

1013 transduced with sh1437 or sh1783 targeting PHOX2B after 4 and 7 days of doxycycline
1014 treatment and compared to untreated cells (100%). GAPDH was used as a reference gene. No
1015 strong changes were observed following PHOX2B decrease. FOSL1, RUNX2 and PRRX1 were
1016 not detected neither in the untreated condition nor after PHOX2B knockdown. TaqMan(r) Gene
1017 Expression Assays (Thermo Fischer Scientific) used in this assays: GAPDH (4326317E),
1018 PHOX2B (Hs00243679_m1), HAND2 (Hs00232769_m1), GATA3 (Hs00231122_m1),
1019 PHOX2A (Hs00605931_mH), FOSL1 (Hs04187685_m1), RUNX2 (Hs01047973_m1), PRRX1
1020 (Hs00246567_m1).
1021
1022
1023
1024
1025
1026
1027
1028
1029
1030
1031
1032
1033
1034
1035
1036
1037
1038
1039
1040
1041
1042
1043

1044

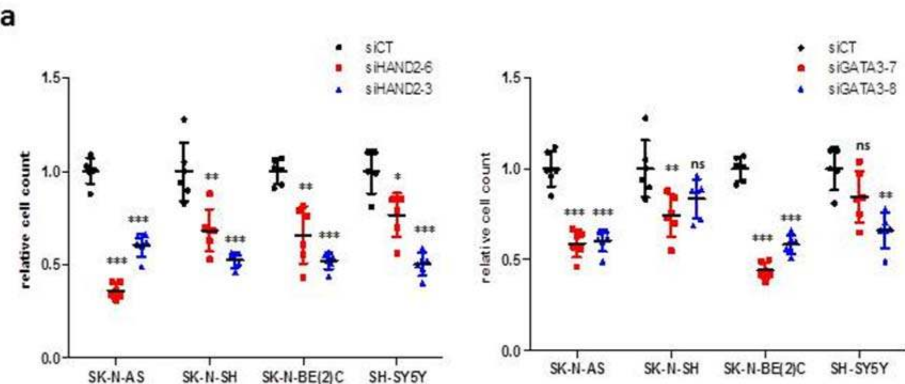

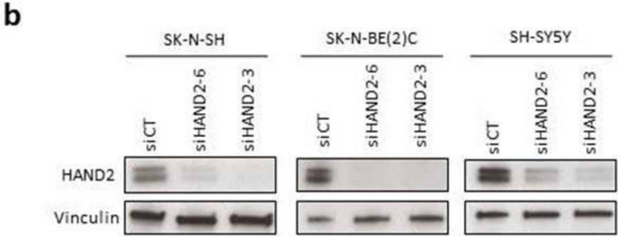

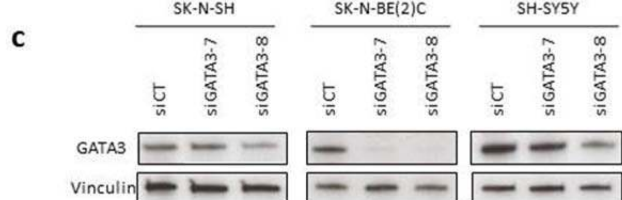

1045
1046
1047

1048 **Supplementary Figure 20:** HAND2 and GATA3 knockdown impairs proliferation of SK-N-
1049 AS, SK-N-SH, SK-N-BE(2)C and SH-SY5Y cell lines. **a**, Cell counting of cells treated with
1050 siRNA targeting HAND2, GATA3 or with a control siRNA (at 3 days post-treatment for SK-N-
1051 BE(2)C, 5 days for SK-N-SH and 6 days for SK-N-AS and SH-SY5Y). (n=5 or 6 technical
1052 replicates, mean +/- s.d.). P values were determined via two-tailed unpaired Welch's t-test (***:
1053 p<0.001). **b and c**, Western blots for HAND2, GATA3, or vinculin.

a

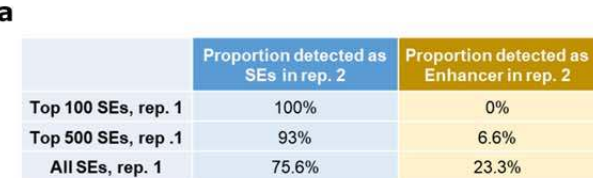

	Proportion detected as SEs in rep. 2	Proportion detected as Enhancer in rep. 2
Top 100 SEs, rep. 1	100%	0%
Top 500 SEs, rep .1	93%	6.6%
All SEs, rep. 1	75.6%	23.3%

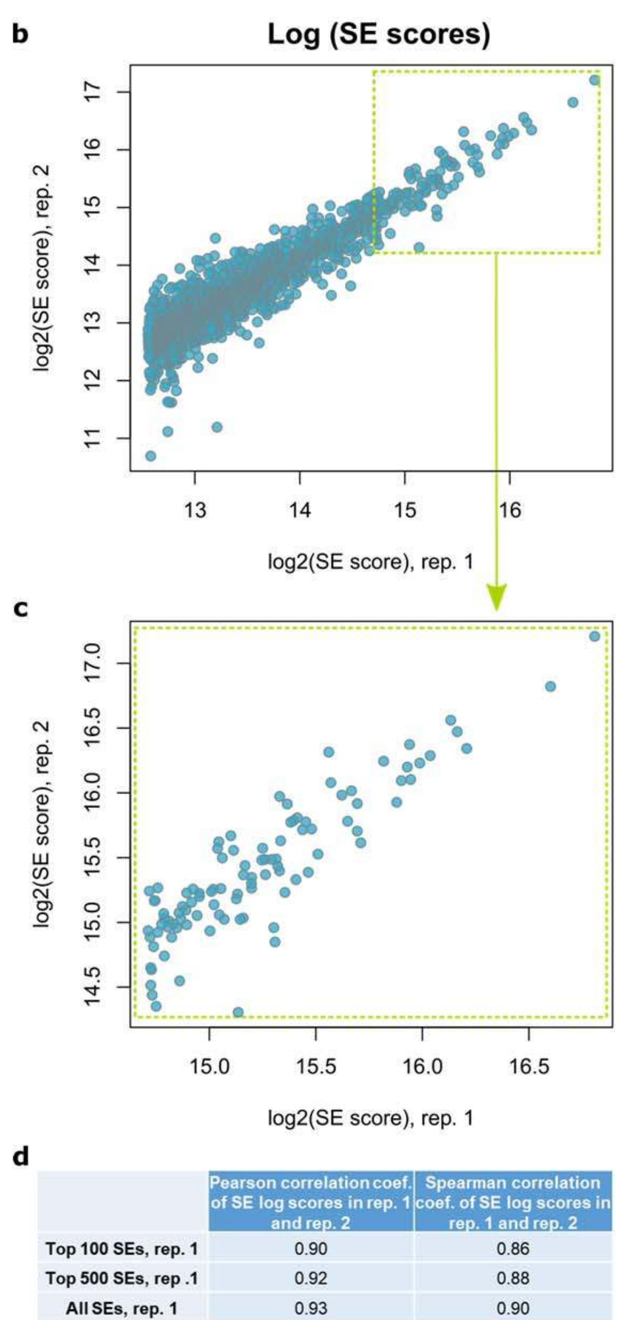

d

	Pearson correlation coef. of SE log scores in rep. 1 and rep. 2	Spearman correlation coef. of SE log scores in rep. 1 and rep. 2
Top 100 SEs, rep. 1	0.90	0.86
Top 500 SEs, rep .1	0.92	0.88
All SEs, rep. 1	0.93	0.90

Supplementary Figure 21: Reproducibility analysis of SE calling and score assessment. ChIP-seq experiment for the H3K27ac mark was performed in duplicate for the CLB-GA cell line. **a**, Proportion of active SEs from replicate 1 detected as SEs in replicate 2. **b**, **c,** Correlation

1058 between normalized values of SE scores in CLB-GA replicate 1 and 2, shown for all the SEs of
1059 replicate 1 (**b**) and the top 100 SEs of replicate 1 (**c**). **d**, Correlation coefficient for SEs scores
1060 between replicate 1 and 2.
1061
1062
1063
1064
1065
1066
1067
1068
1069
1070
1071
1072
1073
1074
1075

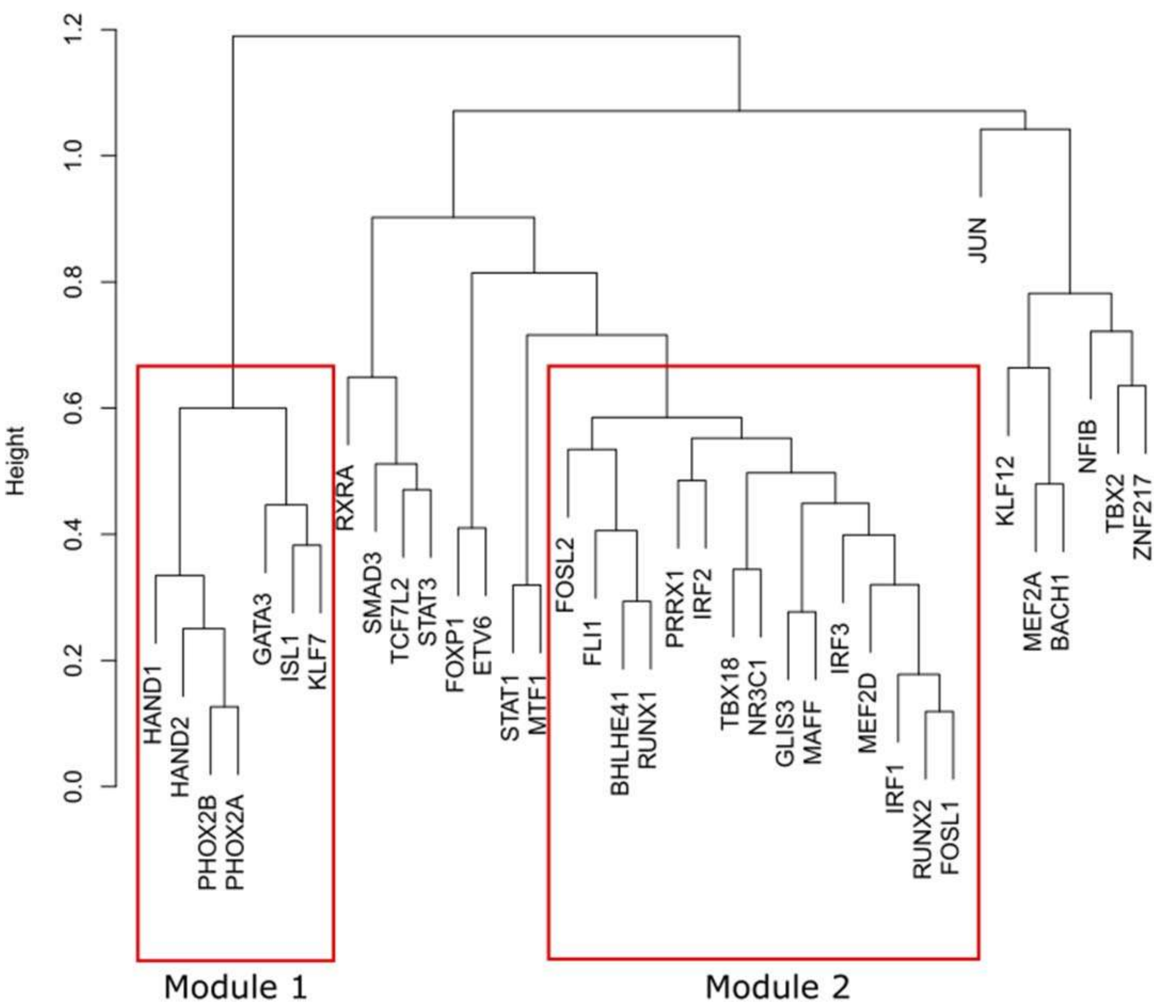

1076

1077 **Supplementary Figure 22:** Clustering of 37 genes from CRCs of neuroblastoma group I and II
1078 based on their expression correlation in NB cell lines and PDX (R package 'hclust' with the
1079 McQuitty method). Two modules were defined.